



HAL
open science

Assessing fluvial organic carbon flux and its response to short climate variability and damming on a large-scale tropical Asian river basin

Clément Fabre, Xi Wei, Sabine Sauvage, Thi Phuong Quynh Le, Sylvain Ouillon, Didier Orange, Marine Herrmann, José-Miguel Sánchez-Pérez

► To cite this version:

Clément Fabre, Xi Wei, Sabine Sauvage, Thi Phuong Quynh Le, Sylvain Ouillon, et al.. Assessing fluvial organic carbon flux and its response to short climate variability and damming on a large-scale tropical Asian river basin. *Science of the Total Environment*, 2023, 903, pp.166589. 10.1016/j.scitotenv.2023.166589 . hal-04278580

HAL Id: hal-04278580

<https://hal.science/hal-04278580>

Submitted on 13 Nov 2023

HAL is a multi-disciplinary open access archive for the deposit and dissemination of scientific research documents, whether they are published or not. The documents may come from teaching and research institutions in France or abroad, or from public or private research centers.

L'archive ouverte pluridisciplinaire **HAL**, est destinée au dépôt et à la diffusion de documents scientifiques de niveau recherche, publiés ou non, émanant des établissements d'enseignement et de recherche français ou étrangers, des laboratoires publics ou privés.

1 **Assessing Fluvial Organic Carbon Flux and its Response to Short**
2 **Climate Variability and Damming on A Large-scale Tropical Asian River**
3 **Basin**

4 Clément Fabre^{a,1}, Xi Wei^{a,1}, Sabine Sauvage^{a*}, Thi Phuong Quynh Le^b, Sylvain
5 Ouillon^{c,d}, Didier Orange^e, Marine Herrmann^{c,d}, José-Miguel Sánchez-Pérez^a

6 ^a Laboratoire Ecologie Fonctionnelle et Environnement, Université de Toulouse,
7 CNRS, INPT, UPS, Avenue de l'Agrobiopole, 31326 Auzeville-Tolosane, France.

8 ^b Institute of Natural Product Chemistry (INPC), Vietnam Academy of Science and
9 Technology (VAST), 100000 Hanoi, Vietnam.

10 ^c LEGOS, Université de Toulouse, IRD, CNES, CNRS, UPS, 31400 Toulouse, France.

11 ^d USTH, Vietnam Academy of Science and Technology (VAST), 100000 Hanoi,
12 Vietnam.

13 ^e HydroSciences Montpellier, Université de Montpellier, CNRS, IMT, IRD, 34095
14 Montpellier, France

15 ¹ These co-authors contributed equally to this work as first authors

16 * Corresponding author: Sabine Sauvage: sabine.sauvage@univ-tlse3.fr

17 **Abstract:**

18 Fluvial organic carbon (OC) transfer is an essential resource for downstream
19 ecosystems. Multiple factors affect its transfer process, e.g., climate or anthropogenic

20 activities. Quantifying OC fluxes with fine spatiotemporal resolution is challenging in
21 anthropised catchments. This study aims to quantify daily OC dynamics and to assess
22 the impacts of short climate variability and damming on OC spatiotemporal transfer
23 processes in a large tropical Asian river basin (the Red River) for an extended period
24 (2003-2013) by combining empirical equations with modelling outputs. Firstly,
25 empirical equations for calculating dissolved (DOC) and particulate OC (POC)
26 concentrations were calibrated based on in-situ sampling data. Then, simulated daily
27 discharge (Q) and suspended sediment concentrations were used to quantify daily
28 OC fluxes. Results show that the parameters of the DOC and POC equations well
29 represent the subbasins characteristics, underlining the effects of soil OC content,
30 mean annual Q and Chlorophyll a. DOC and POC exports reached 222 and 406 kt yr⁻¹
31 at the basin outlet, accounting for 0.38% of the total OC (TOC) exported by Asian
32 rivers to the ocean. However, the specific yields of DOC (1.62 t km⁻² yr⁻¹) and POC
33 (2.96 t km⁻² yr⁻¹) of the Red River basin were ~1.5 times those of other Asian basins.
34 By comparing a reference scenario (without dams) to current conditions, we estimated
35 12% and 88% decreases in DOC and POC fluxes between 2008-2013 and 2003-2007,
36 mainly due to damming. This study shows that climate variability may not impact OC
37 dynamics in rivers as it explained less than 2% of the variations. However, dam
38 management, especially recent ones operating since 2008, deeply influences OC
39 variations as the POC/TOC ratio decreased from 86% to 47%. Damming significantly
40 decreased POC exports due to sediment retention, altering the equilibrium of OC
41 cycling downstream, which may impact the food chain.

42

43 **Keywords:** organic carbon, short climate variability, dam, modelling, Red River.

44

45 **1. Introduction**

46 Rivers are a key connection between terrestrial and marine ecosystems and play an
47 essential role in the global transport of suspended sediment (SS) and associated
48 elements, such as metals, contaminants and nutrients. Fluvial organic carbon (OC) is
49 an essential component in the biogeochemical processes (Bianchi, 2011). It can be
50 classified into two forms: dissolved (DOC) and particulate organic carbon (POC), and
51 is mainly derived from the following three pools: (1) an autochthonous pool derived
52 from in-situ biological production, such as phytoplankton, metabolite of animals and
53 plants in rivers; (2) an allochthonous pool derived from terrestrial organic matter,
54 coming from soil leaching and erosion; (3) an anthropogenic pool derived from
55 agricultural, industrial and domestic release (Hope et al., 1994; Rizinjirabake et al.,
56 2018). Fluvial OC is also regarded as an indicator of water quality (Wen et al., 2019).
57 Metal ions and pesticides can be adsorbed onto OC and carried to the oceans
58 (Boithias et al., 2014; Garneau, 2014). Hence, measuring, quantifying and studying
59 the fate of fluvial OC allows for comprehensively evaluating the degree of organic
60 contamination in water bodies.

61 Tropical humid ecosystems are hot spots of terrestrial carbon storage, and tropical

62 rivers strongly contribute to global fluvial carbon flux (Carvalhais et al., 2014; Huang et
63 al., 2012; Zhang et al., 2019). Ludwig et al. (1996) indicated that about 45% of the OC
64 exported to the oceans originated from tropical wet areas. Based on previous
65 global-scale OC fluxes estimations, the Asian rivers contributed to 36%~67% of the
66 DOC exports (Carlson and Hansell, 2015; Chaplot and Mutema, 2021; Dai et al., 2012;
67 Fabre et al., 2020; Huang et al., 2012; Li et al., 2017; M. Li et al., 2019; Ludwig et al.,
68 1996) and ~50% of the POC exports (Beusen et al., 2005; Huang et al., 2012; Li et al.,
69 2017; Ludwig et al., 1996), with a substantial part coming from anthropogenic sources
70 (Wen et al., 2021). Previous studies also pointed out that the rivers in mainland Asia
71 have the highest specific export rates in terms of DOC and POC (Huang et al., 2012;
72 M. Li et al., 2019; Luo et al., 2022). The Asian monsoon region is identified as a
73 unique and important area to research global carbon dynamics and climate feedback
74 (Fang et al., 2010; Shi et al., 2019; Zhang et al., 2019). Hence, quantifying OC fluxes
75 through tropical Asian rivers is essential further to assess the balance between
76 continental and oceanic fluxes.

77 However, most OC flux estimations were calculated monthly or annually, and hardly
78 any study estimated OC fluxes on a daily time scale. Sampling and modelling are
79 usually performed at fortnightly or monthly intervals, which might induce
80 underestimation when there is a storm or intense rainfall during the intervals since
81 most OC export happens during flood events (Zhang et al., 2019). Hope et al. (1994)
82 indicated that fluvial carbon flux was likely underestimated when studied only based

83 on seasonal data. For most rivers, the OC concentration varies with discharge and
84 season (Coynel et al., 2005). Discharge (Q) is the primary factor controlling the output
85 of OC (Hope et al., 1994), and suspended sediment concentration (SSC) is also the
86 main determinant of POC flux (Boithias et al., 2014; Huang et al., 2012; Ludwig et al.,
87 1996). Q and SSC fluctuate depending on the seasons but also due to intensive daily
88 rainfall and storms, inducing substantial variability of OC concentration and fluxes at
89 the seasonal and daily scales. Therefore, it is essential to develop methods to quantify
90 OC fluxes and their variability from interannual to daily scales to understand OC
91 transport dynamics better and highlight the emergence of hot spots within a
92 catchment.

93 Long-term global changes at the basin scale, such as climate variability and increased
94 damming, have altered carbon biogeochemical cycles (Hope et al., 1994; Hu et al.,
95 2015; Y. Li et al., 2019; Seitzinger et al., 2010). East and Southeast Asia are the major
96 regions influenced by the Asian monsoon and have been considered one of the most
97 critical and sensitive regions in the global climate system (Fang et al., 2010). At the
98 continental scale, the greatest number of large reservoirs and the most significant
99 summed reservoir capacities are located in Asia (Vörösmarty et al., 1997). Future
100 hydropower development is primarily concentrated in developing countries and
101 emerging economies of Southeast Asia (Zarfl et al., 2015). Therefore, understanding
102 the answers of fluvial OC biogeochemical and dynamical processes to those global
103 changes is essential to assess the impact of global changes further. Maavara et al.

104 (2017) showed that current and future OC burial in dams occurs in Asia.

105 In the same way, Liu et al. (2020) showed that reservoir impoundment led to
106 increasing DOC flux and decreasing POC flux in Asia. Nevertheless,
107 catchment-scales studies are needed to understand local consequences of dam
108 implementation. For example, reservoirs impact the POC dynamics in the Yangtze
109 and the Yellow catchments (Liu et al., 2019; Wu et al., 2020; Zeng et al., 2020).

110 The Red River basin is a tropical basin shared among China, Laos and Vietnam,
111 affected by human activities such as intensive agriculture and damming. Previous
112 studies, based on both in-situ sampling data and modelling, have investigated the
113 impacts of human activities on hydrology and SS (Dang et al., 2010; Le et al., 2007;
114 Le et al., 2020; Lu et al., 2015; Vinh et al., 2014; Wang et al., 2011; Wei et al., 2019;
115 2021). These studies especially found strong retention of SS caused by dams.
116 Studies about nutrients associated with Q and SS, such as organic carbon, have also
117 been conducted. Most of these studies analysed the concentrations and fluxes of
118 nutrients based on the sampling data (Dang et al., 2013; Le et al., 2018, 2017a, 2010,
119 2005); few used numerical modelling (Le et al., 2017b; Nguyen et al., 2018). In-situ
120 sampling is a direct and accurate way to quantify fluvial carbon at the local or regional
121 scale. From sampling data, Le et al. (2017a) estimated that the average export of total
122 OC (TOC) during 2008-2010 was 270 kt yr⁻¹ at Hanoi, of which 142 kt yr⁻¹ was DOC,
123 and 128 kt yr⁻¹ was POC; Dang et al. (2013) quantified the annual POC flux of 243 kt
124 yr⁻¹ at Son Tay during 2006-2009 (see Figure 1 for sampling locations). However,

125 in-situ field sampling at large spatial and temporal scales is expensive and often
126 impracticable. Combined with available in-situ data, a numerical modelling approach
127 allows for overcoming these shortages. Le et al. (2017b) and Nguyen et al. (2018)
128 used a modelling approach to identify a seasonal OC variation and estimated a TOC
129 export of 324 kt yr⁻¹ at Son Tay during 2013-2014. However, as explained above,
130 simulations at a seasonal scale do not represent the whole range of OC flux variability
131 and might induce underestimations (Hope et al., 1994). Therefore, assessing and
132 calculating OC flux at a daily time step would be more precise using daily Q, SSC and
133 OC concentrations.

134 This work aims to understand the DOC and POC transport dynamics and quantify
135 DOC and POC fluxes and variabilities based on a daily time step through the Red
136 River basin. The specific objectives of this paper are: (1) to quantify DOC and POC
137 fluxes through the basin during a long-term period (2003-2013) on a daily time step; (2)
138 to assess the influence of short climate variability and damming on DOC and POC
139 transport and fluxes; (3) to propose a new approach to evaluate DOC and POC at
140 different points in the basin with accessible environmental parameters.

141

142 **2. Materials and Methods**

143 **2.1. Study area**

144 The Red River basin covers a total area of approximately 159,000 km². Our study
145 area focuses on the continental drainage catchment at Son Tay, which is also the

146 apex of the delta, resulting in a surface of 137,200 km² (Figure 1).

147 The Red River is comprised of three main tributaries: the upper part of the main river
148 before the confluence (the Thao River), which is the current main sediment load
149 contributor (~80%) to Son Tay (Le et al., 2007; Vinh et al., 2014; Wei et al., 2021); the
150 Da River, on the right river bank; the Lo River, on the left riverbank (Figure 1).

151 The elevation in the basin ranges from 20m to 3000m. Most areas are mainly
152 mountainous, with slopes mainly above 6%. The upper part of the Red River basin is
153 formed by tectonically active mountains vulnerable to high erosion with intensive
154 rainfall (Bai et al., 2015; Barton et al., 2004; He et al., 2007; Wei et al., 2021).

155 Land use is presented in Figure 2. Forest and agriculture account cover most of the
156 Red River basin. Land use change during 2000-2010 was insignificant, as only less
157 than 4% of the bare land in the Red River basin was converted to agricultural land (Le
158 et al., 2018).

159 Concerning the hydrological cycle, the whole Red River basin is influenced by the
160 monsoon system, from the humid subtropical monsoon in the upstream basin to the
161 humid tropical monsoon in the downstream part, and associated with strong
162 seasonality. The mean annual rainfall is 1590 mm in the Red River basin, and over
163 85-90% of the yearly precipitation falls during the southwest monsoon season (May to
164 October; Le et al., 2007; Li et al., 2016). The rainfall is unevenly distributed (Li et al.,
165 2008; Luu et al., 2010; Xie, 2002). Runoff shows high inter-seasonal variations, with a
166 flood season occurring between May and October, with over 80% of the total annual

167 runoff. The discharge at Son Tay is about $3,000 \text{ m}^3 \text{ s}^{-1}$, with floods exceeding 20,000
168 $\text{m}^3 \text{ s}^{-1}$ (Vietnam Ministry of Natural Resources and Environment; MONRE). The
169 annual water volumes within the catchment are 20.7, 28.2, 51.9, and $99.0 \text{ km}^3 \text{ yr}^{-1}$ at
170 Yen Bai, Vu Quang, Hoa Binh and Son Tay stations, respectively.

171 Concerning suspended matter, sediment fluxes were strongly affected by the
172 construction of dams (Le et al., 2007; Lu et al., 2015; Vinh et al., 2014; Wei et al.,
173 2021). This basin has six important dams with large storage capacities (Figure 1). The
174 two dams on the Thao River started operating in 2008 and 2011. The two dams on the
175 Lo River were impounded in 1972 and 2008. Two larger dams on the Da River started
176 to operate in 1989 and 2011. More details about these dams can be found in Wei et al.
177 (2019).

178 **2.2. Data sources**

179 Daily Q and SSC data were obtained from the Vietnam Ministry of Natural Resources
180 and Environment at Yen Bai, Vu Quang, Hoa Binh and Son Tay stations from 2003 to
181 2013 (see Figure 1).

182 Modelling inputs such as topography (digital elevation model), land use, soil map,
183 rainfall and temperature were used to simulate daily Q and SSC using the Soil and
184 Water Assessment Tool (SWAT; Neitsch et al., 2009), as detailed in the previous work
185 of Wei et al. (2019). Land use and soil map are presented in Figure 2.

186 POC and DOC data come from Dang (2011) and Le et al. (2017a). Dang (2011)
187 provided POC and DOC concentrations at Yen Bai, Vu Quang, Hoa Binh and Son Tay

188 during 2008-2009, with sampling frequency generally monthly or bimonthly. POC was
189 determined using a LECO CS 125 analyser, and DOC was measured with a TOC
190 5000 Shimadzu. Analytical accuracy was evaluated between 3 and 5 % (Dang et al.
191 (2010).

192 Le et al. (2017a) sampled DOC and POC one to three times per month from
193 2003-2004, 2008-2010, and 2012-2013 at Yen Bai, Vu Quang, Hoa Binh and Son Tay.
194 Due to the sampling difficulties, data are missing for some years or months. In the
195 same way, POC was measured with a LECO CS 125 analyser, while DOC was
196 determined with an ANATOC II TOC analyser. Detailed information about these
197 sampling and laboratory measurements can be found in Dang (2011) and Le et al.
198 (2017a).

199 **2.3. Organic carbon calculation**

200 2.3.1. DOC equation

201 The equation for calculating the DOC concentration [DOC] from daily Q was taken
202 from the work of Fabre et al. (2019):

$$203 \quad [\text{DOC}] = \frac{\alpha * Q}{\beta + Q} \quad (1)$$

204 where [DOC] is in mg L^{-1} , Q in mm d^{-1} ; the parameter α (mg L^{-1}) represents a potential
205 of maximum [DOC] at the outlet of each sub-basin, and the parameter β (mm d^{-1}) is
206 the Q when [DOC] is half of α .

207 2.3.2. POC equation

208 The equation for calculating the POC concentration was proposed by Boithias et al.

209 (2014), who generalised the relation between the POC and suspended sediment
210 concentration (SSC) as follows:

$$211 \quad \begin{cases} \%POC = \frac{9.40}{SSC-a} + b \text{ (if } SSC > a) \\ \%POC = \%POC_{max} \text{ (if } SSC \leq a) \end{cases} \quad (2)$$

212 where %POC is the percentage of POC in the suspended sediment, %POC_{max} is the
213 maximum value over the basin, SSC is in mg L⁻¹, and parameters *a* and *b* are linked to
214 environmental variables related to each sub-basin (see details in section 3.1.4). The
215 parameter *a* (in mg L⁻¹) is the vertical asymptote corresponding to a low SSC with
216 organic matter rich in OC, such as phytoplankton and residuals. The parameter *b*
217 (in %) is the horizontal asymptote representing the suspended matters with low OC
218 concentration, nearly equals to soil organic carbon content (Boithias et al., 2014;
219 Fabre et al., 2019). When SSC is smaller than *a*, %POC equals its maximum
220 value, %POC_{max}.

221 **2.4. Modelling strategy**

222 2.4.1. Parameters calibration for DOC and POC

223 The four parameters (α , β , *a*, *b*) in Equations 1 and 2 were manually calibrated based
224 on the discrete OC sampling data and the observed daily Q and SSC at each station.
225 It allowed determining values of specific parameters associated with each sub-basin,
226 which are representatives of the characteristics of these sub-basins. The values of
227 each parameter were calibrated separately in order to obtain simulated values as
228 close as possible to the observed values. The maximum value of %POC was set by
229 considering covering 99.9% of the dataset.

230 2.4.2. Scenarios setting

231 The SWAT is a physically-based model used to simulate the quality and quantity of Q,
232 SSC and nutrients over the river basin and to predict the environmental impacts of
233 human activities and short climate variability (Neitsch et al., 2009). The version of
234 SWAT we used in this study (SWAT 2012) cannot compute the DOC and POC
235 concentrations. Wei et al. (2019) applied the SWAT model on the Red River, obtaining
236 simulated daily Q and SSC from 2000 to 2013 in good agreement with in-situ
237 measurements (scenario of current conditions, with dams). A reference scenario
238 (without dams) was also implemented to assess separately the impacts of short
239 climate variability and dams on Q and SSC, respectively. Current conditions and
240 reference scenario settings are presented in Figure 3. More detailed information on
241 simulated Q and SSC can be found in Wei et al. (2019).

242 This study aims to apply the simulated daily Q and SSC of the current conditions and
243 the reference scenario (without dams) to calculate the simulated DOC and POC
244 fluxes under those conditions (Figure 3).

245 **2.5. Model evaluation and validation for DOC and POC**

246 The simulated OC fluxes of current conditions from modelling would be validated by
247 comparing them to the results from the Load Estimator (LOADEST) regression model,
248 which U.S. Geological Survey developed for estimating constituent loads in rivers
249 (Runkel et al., 2004) and had been applied to many studies (Huntington and Aiken,
250 2013; McClelland et al., 2007; Sickman et al., 2007; Tamm et al., 2008). Daily water
251 releases and OC concentrations are available in both high and low flow periods, which

252 makes the LOADEST approach consistent. LOADEST model will provide a more
253 consistent dataset of data based on observed values, which will allow calculating
254 monthly observed fluxes. LOADEST model is calibrated through regression analysis
255 based on discrete OC sampling data and observed daily Q. The best regression
256 model (Approximate Maximum Likelihood Estimator) is used with LOADEST to
257 estimate daily DOC and POC fluxes, respectively. The mean annual DOC and POC
258 fluxes from other studies in the same basin (Dang, 2011; Le et al., 2017a) were also
259 used as references for validating the simulations from this study.

260 The coefficient of determination (R^2) and the Nash–Sutcliffe efficiency (NSE) were
261 used as statistical tests to evaluate the quality of our calculation by comparing the
262 results from LOADEST with ours (Moriassi et al., 2007; Nash and Sutcliffe, 1970). R^2
263 values greater than 0.3 or 0.4 are considered satisfactory for monthly nitrogen or
264 sediment loads, respectively (Moriassi et al., 2015). NSE values greater than 0.35 and
265 0.45 are generally considered satisfactory for monthly nitrogen or sediment loads,
266 respectively (Moriassi et al., 2015). We assumed we could use these thresholds for
267 organic carbon studies.

268 **3. Results**

269 **3.1. DOC and POC concentrations**

270 3.1.1. DOC equation application

271 The value of parameters α and β in Equation 1 obtained for each station and the
272 number of sampling DOC used for inferring the parameters are listed in Table 1. The

273 values of parameter α vary from 4.5 to 5.5; parameter β ranges from 0.7 to 2.5,
274 geographically increasing from the upstream to the downstream.

275 3.1.2. DOC concentrations temporal variations

276 The daily variations of observed and simulated DOC concentrations at four stations
277 from 2003 to 2013 are presented in Figure 4. The observed DOC concentrations were
278 measured over some short periods and did not show apparent seasonal variations.
279 The simulated DOC concentrations are in the range of the observations (values of the
280 range are presented in the following sub-section), with most sampling points captured
281 by our simulations. Generally, simulated DOC concentration varies following Q
282 variations, increasing from May to July, staying high during the highest floods in
283 August and September, and decreasing from October to April.

284 Simulated mean annual DOC concentrations increase in the following order: Yen Bai
285 (1.39 mg L^{-1}) < Vu Quang (1.50 mg L^{-1}) < Hoa Binh (1.60 mg L^{-1}) < Son Tay (1.81 mg
286 L^{-1}).

287 3.1.3. DOC concentration ranges and spatial variations

288 Simulated DOC concentrations at four stations varied slightly (Figure 5a). At Yen Bai
289 station, DOC concentration ranges from 0.01 to 4.13 mg L^{-1} with an average of 1.25
290 mg L^{-1} (observations from 0.20 to 5.90 mg L^{-1}); at Vu Quang, DOC was in the range of
291 0.03 to 4.01 mg L^{-1} with an average of 1.50 mg L^{-1} (observations from 0.33 to 5.70 mg
292 L^{-1}); at Hoa Binh, DOC concentration varied from 0.05 to 4.05 mg L^{-1} with an average
293 of 1.60 mg L^{-1} (observations from 0.12 to 5.65 mg L^{-1}); at Son Tay, DOC shifted from

294 0.05 to 4.11 mg L⁻¹ with an average of 1.81 mg L⁻¹ (observations from 0.36 to 6.00 mg
295 L⁻¹).

296 3.1.4. POC equation application

297 Figure 6 shows the percentage of POC in suspended sediment (%POC) against the
298 suspended sediment concentration (SSC) computed from available measurements in
299 2003-2013. %POC shows a significant negative relationship with SSC, following well
300 Equation 2.

301 We obtained different values for the parameters *a*, *b*, and %POC_{max} for the four
302 stations (Table 1). The parameter *a* varies broadly, with a maximum value of 40.0 mg
303 L⁻¹ at Yen Bai and a minimum of 5.0 mg L⁻¹ at Hoa Binh. Parameter *b* varies from 1.0
304 to 1.7%, with a maximum at Hoa Binh and a minimum at Yen Bai. %POC_{max} varies
305 strongly, with a minimum of 10 mg L⁻¹ at Yen Bai and a maximum of 40 mg L⁻¹ at Hoa
306 Binh.

307 3.1.5. POC concentrations temporal variations

308 Figure 7 illustrates the daily variations of simulated and observed POC concentrations
309 at four stations from 2003 to 2013. POC concentrations showed great seasonal and
310 inter-annual variations. POC peak flows occurred from May to October. Seasonal
311 variations strongly weakened during more recent years (2008-2013), and the POC
312 peak flows decreased. For Yen Bai, Vu Quang, Hoa Binh and Son Tay stations, the
313 standard deviation is 10.11, 2.75, 0.84, and 3.55 mg L⁻¹, respectively, over 2003-2007,
314 and 3.76, 0.83, 0.53, and 0.96 mg L⁻¹, over 2008-2013; and the maximum POC

315 concentration is 82.77, 18.86, 7.91, 22.72 mg L⁻¹ during 2003-2007 and 30.12, 9.50,
316 12.31, and 6.52 mg L⁻¹ respectively during 2008-2013.

317 Simulations are in the same range as discrete samplings (values of the range are
318 presented in the following sub-section) and produce acceptable results. Comparing
319 the simulated POC concentrations to the observations, simulated POC peaks can be
320 underestimated for some years. Simulated POC base values are generally in good
321 agreement with in-situ observations.

322 3.1.6. POC concentration ranges and spatial variations

323 Figure 5b presents the simulated POC concentration ranges at the four stations. From
324 the simulations, POC concentrations vary from 0.85 to 82.77 mg L⁻¹ with an average
325 of 8.35 mg L⁻¹ at Yen Bai (observations from 0.14 to 67.20 mg L⁻¹), from 0.40 to 18.86
326 mg L⁻¹ with an average of 2.30 mg L⁻¹ at Vu Quang (observations from 0.20 to 5.17 mg
327 L⁻¹), from 0.36 to 12.31 mg L⁻¹ with an average of 0.96 mg L⁻¹ at Hoa Binh
328 (observations from 0.18 to 3.27 mg L⁻¹) and from 0.43 to 22.72 mg L⁻¹ with an average
329 of 3.03 mg L⁻¹ at Son Tay (observations from 0.20 to 23.78 mg L⁻¹). Our simulations
330 have larger ranges compared to observations because our simulations period covers
331 the years before dam implementation when the POC concentrations were high. The
332 POC low concentrations at these four stations do not differ much, but significant
333 differences occur at POC peak fluxes.

334 3.2. Fluxes of DOC and POC

335 3.2.1. DOC flux variations

336 Daily variations of DOC fluxes at four stations are presented in Figure 8a. Simulated

337 DOC fluxes fit well with the observations during low flow periods. Daily simulations
338 represent the DOC flux fluctuations realistically during flood seasons.

339 As described in section 2.5, the LOADEST model results are used as references to
340 validate our simulations. Figure 8b shows the DOC fluxes from LOADEST and our
341 simulations at a monthly scale. Compared to the results from LOADEST, the
342 simulated base DOC flux is lower, and the peak DOC flux is higher for some years;
343 the R^2 at these four stations varies from 0.65 to 0.74, and the NSE is in the range of
344 0.02-0.56, which indicates that our simulations of DOC fluxes at monthly scale are
345 acceptable to good. At Son Tay outlet, 85% of the total export of DOC happened in the
346 southwest monsoon seasons (from May to October).

347 Annual DOC simulated fluxes variations are presented in Figure 9. The mean annual
348 DOC flux during the study period at Yen Bai, Vu Quang, Hoa Binh and Son Tay
349 stations are 44, 53, 88 and 222 kt yr^{-1} , respectively. The maximum annual DOC flux
350 occurred in 2008, the maximum flood year during the study period. The minimum
351 annual DOC flux occurred in 2010, the drier year during the study period.

352 3.2.2. POC flux variations

353 Figure 10a illustrates the daily variations of POC fluxes at four stations. As for daily
354 DOC fluxes, simulated POC fluxes are in the range of the observations.

355 The observed data were sampled after 2007, and some dams (the Nansha,
356 Madushan, Tuyen Quang and Son La dams) were under construction during the
357 2003-2007 period and have been operating since 2008. The POC conditions before

358 and after 2008 were hence different because of the impacts of dam constructions on
359 suspended sediment. The POC sampling concentrations before 2008 are few and
360 limited. Here we thus only compared the POC fluxes from LOADEST and our
361 simulation over the 2008-2013 period. Our simulation results during 2003-2007 were
362 plotted to provide insight into POC fluxes during this period (Figure 10b). Generally,
363 the results from LOADEST and our simulation fit well on both POC peak and base
364 fluxes: R^2 is between 0.50-0.59, while NSE varies from 0.34 to 0.56, indicating a
365 satisfactory performance. At Son Tay, 88% of the total POC fluxes are exported to the
366 delta from the southwest monsoon season.

367 Figure 11 shows the simulated annual POC flux variations for the four stations
368 between 2003-2013. The mean annual POC fluxes of Yen Bai, Vu Quang, Hoa Binh
369 and Son Tay stations are 318, 83, 55 and 406 kt yr^{-1} , respectively. The Thao River
370 exported the highest POC loads among the three tributaries, followed by the Lo River.
371 Contrary to what was obtained for the DOC export, the Da River exported the smallest
372 POC flux. The POC flux was the highest at the confluence (Son Tay station). The
373 maximum annual POC flux generally occurred in 2007, while the minimum annual
374 POC flux occurred in 2011.

375 3.2.3. Spatial variations of new dams impacts on DOC and POC dynamics

376 The effects of dams implementation on each main tributary were assessed by
377 comparing values obtained during the period 2003-2007 and the period 2008-2013.
378 Table 2 shows the effects of the new dams on OC dynamics. New dams induce a

379 spatially homogeneous decrease between 64 and 71% for POC while it shows slight
380 variations (between -9% and +5%) for DOC.

381 Concerning the contribution of the main tributaries to the outlet, the implementation of
382 the new dams seems not to impact the balance of the contributions by the tributaries.
383 For POC, the Thao River is responsible of 70% of the export followed by the Lo River
384 with about 20% and by the Da River with 10%. For DOC, the main contributor is the
385 Da River with 46% of the exports, followed by the Lo River with 30% and by the Thao
386 River with 24% of the exports.

387 3.2.4. TOC flux variations

388 Annual simulated TOC fluxes showed significant inter-annual variations (Figure 12).
389 The mean annual TOC fluxes for the study period were 350, 136, 143 and 628 kt yr⁻¹
390 at Yen Bai, Vu Quang, Hoa Binh and Son Tay stations, respectively. Comparing the
391 TOC export among the three tributaries, TOC fluxes exported by the Lo and Da rivers
392 were of the same order, and the Thao River exported around 2.5 times higher TOC
393 than the Lo and Da rivers. The highest TOC fluxes were generated in 2007 and the
394 lowest in 2010.

395 **3.3. TOC fluxes variations under the reference scenario**

396 Figure 13a presents simulated monthly TOC flux variations under the reference
397 scenario and current conditions at Son Tay station. The differences between the
398 reference scenario and current conditions for monthly DOC fluxes are slight ($p=0.5$),
399 while they are significant for monthly POC fluxes ($p<0.001$). The differences in the

400 dynamic processes between the reference scenario and current conditions occur
401 during the flood seasons and are much more significant for POC than DOC: the
402 average monthly fluxes during June and August under the reference scenario and
403 current conditions for DOC are 42.0 and 40.3 kt month⁻¹. They are 271.5 and 72.4 kt
404 month⁻¹ for POC.

405 The annual fluxes of POC under the reference scenario and current conditions also
406 differ considerably compared to the DOC fluxes (Figure 13b). When comparing the
407 period after new dams (2008-2013) to the previous period (2003-2007), the annual
408 DOC flux was reduced by 12%: a 1% increase due to Q change induced by short
409 climate variability and a 13% decrease due to dam constructions. The annual POC
410 flux decreased by 87%, of which 2% was due to Q variation caused by short climate
411 variability and 85% due to damming. POC variations resulted in the variations of POC
412 percentage in TOC (POC/TOC) at Son Tay station (Figure 14).

413 The POC/TOC ratio under the reference scenario is higher (from 81 to 89% with an
414 averaged value of 85%, standard deviation=1.7%) than that under current conditions
415 (from 33 to 90% with an averaged value of 58%, standard deviation=13.6%);
416 moreover, the POC/TOC ratio under reference scenario shows a weaker seasonal
417 variability than under current conditions (Figure 14a).

418 The ratio POC/TOC under current conditions decreased after 2007, and its seasonal
419 variability also changed afterwards (Figure 14a). During 2003-2007, the maximum
420 POC/TOC generally occurred in September and October, whereas the minimum

421 POC/TOC showed up during February and March. During 2008-2013, the maximum
422 POC/TOC showed up generally in February and March and the minimum in
423 December, January or June.

424 There is a clear negative POC/TOC ratio shift in 2008 under current conditions (Figure
425 14). The mean annual POC/TOC ratio under the reference scenario stayed the same
426 (86%) during 2003-2007 and 2008-2013, while under current conditions, it decreased
427 from 74% during 2003-2007 to 47% during 2008-2013.

428 **4. Discussion**

429 **4.1. Parameter analysis**

430 4.1.1. Parameters of DOC

431 The parameter α is the potential maximum fluvial DOC concentration at each station,
432 and it can be related to its sources. Previous studies indicated that DOC increased
433 with increasing soil carbon content (Manninen et al., 2018). The soil organic matter,
434 through soil erosion and leaching, was the main source of fluvial DOC (Dang, 2011;
435 Le et al., 2017a; Lloret et al., 2016). Figure 15a presents the soil organic carbon
436 content through the Red River basin. The average soil organic carbon contents (%
437 soil weight) of the drainage area of Yen Bai, Vu Quang, Hoa Binh and Son Tay are
438 1.60%, 1.79%, 1.92% and 1.77%, respectively. Figure 15b shows that the relationship
439 between the parameter α and the average soil organic carbon content of the drainage
440 area of each station is significant, indicating a positive correlation. The increasing
441 order of mean annual DOC concentration during 2003-2013 at the outlet of each river

442 is consistent with the increasing order of the average soil organic carbon content: Yen
443 Bai < Son Tay < Vu Quang < Hoa Binh.

444 The parameter β corresponds to the discharge Q when the DOC concentration is half
445 of α , so it is linked to α . Besides, β increases in the following order: Yen Bai < Vu
446 Quang < Hoa Binh < Son Tay (Table 1), and the annual mean Q for these four stations
447 (Yen Bai: $608 \text{ m}^3 \text{ s}^{-1}$, Vu Quang: $848 \text{ m}^3 \text{ s}^{-1}$, Hoa Binh: $1529 \text{ m}^3 \text{ s}^{-1}$, Son Tay: 3052 m^3
448 s^{-1}) increase in the same order. We assume that within the same basin, the parameter
449 β can be positively correlated with Q. However, this needs further study and
450 confirmation from other basins worldwide.

451 Equation 1 was also applied at the outlet of the Yenisei River basin, located in the
452 Arctic region with a watershed surface of $2,540,000 \text{ km}^2$. The parameters α and β
453 were 15.0 and 1.29, respectively (Fabre et al., 2019). The α at the outlet of the Yenisei
454 River basin is higher than at the Red River outlet due to the high soil OC contents in
455 the Yenisei basin. It agrees with the relationship between the parameter α and the soil
456 organic carbon content (% soil weight; Figure 15).

457 4.1.2. Parameters of POC

458 The maximum %POC decreases in the following order (Table 1): Hoa Binh (40) \geq
459 Son Tay and Vu Quang (15) > Yen Bai (10). The SSC at Hoa Binh station was the
460 lowest (annual mean during 2003-2013 is 34 mg L^{-1}) compared to other stations
461 (annual mean SSC for Yen Bai, Vu Quang, and Son Tay is 631, 99 and 137 mg L^{-1} ,
462 respectively) due to the retention by the dams, especially by the Hoa Binh dam (Dang

463 et al., 2010; Wei et al., 2019). Besides, algae and phytoplankton in the reservoir can
464 contribute to high particulate organic carbon. Therefore, these two factors induce a
465 high maximum %POC at Hoa Binh station. On the contrary, at Yen Bai station, the
466 SSC is the highest with low autochthonous organic production compared to other
467 stations (Dang et al., 2010; Dang, 2011; Nguyen et al., 2018). Therefore, the
468 maximum %POC is small.

469 The parameter a is a basin-specific constant that includes anthropogenic impacts and
470 corresponds to low SSC values and to matter rich in OC, such as phytoplankton and
471 residuals. Comparing the minimum SSC values of the three tributaries, the Thao River
472 presents the highest concentration (15.2 mg L^{-1}). In contrast, at Hoa Binh station on
473 the Da River, the lowest concentration (0.6 mg L^{-1}) is observed, which explains the
474 corresponding values of a - high at Yen Bai (40, Table 1) and low at Hoa Binh (5).
475 Besides, thanks to the Nansha and Madushan dams constructions, local villagers
476 have entered into extensive fish farming (Rousseau, 2014), while fish feed and faeces
477 are rich in organic matter (Beristain, 2005). Moreover, near the Nansha dam, a
478 sugarcane processing plant often releases chemicals and wastes into the Red River
479 (Rousseau, 2014). These factors make the water quality downstream of the
480 Madushan dam very bad (Rousseau, 2014), which contributes to explaining the high
481 parameter a value at Yen Bai. In addition, the concentrations of Chl- a of these three
482 tributaries from large to small was in the following order: Yen Bai ($1.9 \text{ } \mu\text{g L}^{-1}$) > Vu
483 Quang ($1.3 \text{ } \mu\text{g L}^{-1}$) > Hoa Binh ($1.1 \text{ } \mu\text{g L}^{-1}$; no data for Son Tay in Le et al., 2017a),

484 which is in the same order as the values of parameter *a* (Figure 15d). Therefore, the
485 parameter *a* accurately expresses the characteristics of each tributary in this study.

486 As described in subsection 2.3.2, parameter *b* is the horizontal asymptote
487 representing the suspended matters with low OC concentration near soil content.
488 From Figure 15e, we can see that parameter *b* shows a positive and significant
489 correlation with the average soil organic carbon content of the drainage area of each
490 station. Hence, the values of the parameter *b* well represent the characteristics of
491 each sub-basin.

492 The parameters *a* and *b* were set to 5 mg L⁻¹ and 2.1%, respectively, in an agricultural
493 basin in southeast France (Boithias et al., 2014); and to 0.95 mg L⁻¹ and 3.9%,
494 respectively in an Arctic basin (Fabre et al., 2019). The minimum SSC observed in the
495 study river of Boithias et al. (2014) is 5 mg L⁻¹, while it is around 1 mg L⁻¹ of Fabre et al.
496 (2019); hence, they set the parameter *a* to 5 mg L⁻¹ and 0.95 mg L⁻¹. In our study, the
497 parameter *a* is higher than the minimum SSC observed at each station, which
498 indicates the contributions from phytoplankton and residuals in the Red River that
499 were not observed in the study rivers of Boithias et al. (2014) and Fabre et al. (2019).

500 In the study area of Boithias et al. (2014), the topsoil organic matter content is about
501 2%, which is higher than our basin (1.6-1.9%). In the study case of Fabre et al. (2019),
502 the permafrost stores abundant soil OC, leading to a high parameter *b*. Therefore, the
503 parameter *b* from their study is higher than ours (from 1.0% to 1.7%). From the above,
504 the parameters *a* and *b* obtained from Boithias et al. (2014), Fabre et al. (2019), and

505 this study seem to represent the specific characteristics of various local basins.

506 4.1.3. Application: a new method to evaluate the DOC and POC concentrations

507 Our results also enable us to propose a new method to evaluate the DOC and POC

508 concentrations at any point within the Red River basin. If one knows the values of

509 average soil organic carbon content of the drainage area, mean annual discharge and

510 the Chl-a concentration in the river, using the relationships in Figure 15 allows to

511 determine α , β , a and b ; Equation 1 and 2 can then be used to evaluate the DOC and

512 POC concentrations.

513 **4.2. Comparison of the OC contents with other studies**

514 4.2.1. Comparison with other studies for the Red River

515 We first compared our simulations with results from other studies based on in-situ

516 sampling in the Red River basin (Table 3). To make things comparable, we performed

517 our comparison over the 2008-2009 period.

518 Our simulated results are slightly lower (about -17%) for the mean annual DOC

519 concentration compared to the other two studies (Dang, 2011; Le et al., 2017a). In

520 both studies, discrete samplings were just taken once or twice per month, and at dry

521 seasons the frequency was even lower, while our results were calculated based on a

522 daily time step simulation. Those different temporal scales can induce differences in

523 mean annual DOC concentration estimations. The mean yearly DOC flux of

524 2008-2009 at Vu Quang and Hoa Binh stations estimated by Dang (2011) is around

525 60% higher than that of Le et al. (2017a). Note that the LOADEST results are close to

526 the ones of Le et al. (2017a; Table 3) as a large proportion of sampling data used by

527 the LOADEST comes from their dataset. Comparing our results to the LOADEST, the
528 DOC fluxes are 17-28% higher at the three tributaries and 3% higher at the outlet Son
529 Tay station. Hope et al. (1994) indicated that low-frequency sampling led to
530 underestimating the fluvial carbon flux due to the under-representation of storm flow
531 conditions. Finally, our study produces an estimation of 222 kt yr^{-1} of DOC flux at Son
532 Tay (Table 3) over 2003-2013, which accounts for 0.26% of the total DOC export by
533 Asian rivers to the seas, estimated to 85.45 Mt yr^{-1} by Li et al. (2019).

534 Significant differences in mean annual POC concentration during 2008-2009 can be
535 found between Dang (2011) and Le et al. (2017a): POC concentrations from Le et al.
536 (2017a) are only 31% of that from Dang (2011); our results are between theirs (Table
537 3). POC concentrations are strongly linked to SSC, which can vary significantly from
538 sampling location and time. Le et al. (2017a) estimated that the POC fluxes are about
539 59% of the values Dang (2011) estimated, especially at Yen Bai station, where the
540 SSC is very high. Comparing our results to the LOADEST, our estimations are 10-31%
541 lower on the three tributaries and 34% lower at Son Tay. Since POC fluxes
542 transported by the Asian rivers are 76.90 Mt yr^{-1} (Li et al., 2017), the export of POC at
543 Son Tay (406 kt yr^{-1} over 2003-2013 in our study) accounts for 0.37% of the total POC
544 export by the Asian rivers.

545 The estimated TOC flux during 2003-2013 at Son Tay equals 628 kt yr^{-1} . Regardless
546 of the time, the mean annual TOC at Son Tay was estimated from 324 to 506 kt yr^{-1}
547 (Dang, 2011; Nguyen et al., 2018), and our simulation is higher than theirs (94%

548 higher than Nguyen et al. (2018) and 24% higher than Dang (2011), again due to the
549 difference of calculation time step: our simulations at a daily time step consider all
550 flood events. Finally, our results suggested that the Red River exported 628 kt yr^{-1} of
551 TOC over 2003-2013, i.e. contributed approximately 0.38% of TOC exported by the
552 Asian rivers (164 Mt yr^{-1} , Li et al., 2017).

553 4.2.2. Comparison with other rivers

554 Compared with other Asian and tropical rivers, the exports of DOC and POC through
555 the Red River are not that large, especially for POC (Table 3). However, when
556 comparing specific yields, the Red River basin yields high DOC and POC values. It is
557 in agreement with some previous studies, indicating that the rivers in mainland Asia,
558 especially those originating from the Himalayan plateau, have the highest specific
559 POC and DOC export rates worldwide (Aucour et al., 2006; Galy et al., 2007; Huang
560 et al., 2012; M. Li et al., 2019).

561 The DOC flux of the Red River is 58% and 10% higher than that of the Pearl and
562 Mekong Rivers, respectively, which are geographically close to the Red River (Table
563 3). In the same way, the DOC exports of the Red River are 14%, 171% and 370%
564 higher than that of the Yangtze, Godavari and Yellow Rivers. Compared to other large
565 rivers, the specific fluxes are in the same range as that of the Amazon and Congo
566 rivers, the two largest basins in the world.

567 However, the DOC yield of the Red River basin ($1618 \text{ kg km}^{-2} \text{ yr}^{-1}$) is about twice that
568 of the Pearl and Yangtze basins and around half that of the Mekong and Congo

569 basins (Table 3). Though the DOC flux of the Red River is smaller than those of the
570 Pearl and Yangtze Rivers, its specific DOC yield is higher than theirs. The high DOC
571 yield of the Red River basin comes from high leaching from soil and rocks. Previous
572 studies pointed out that the DOC in the Red River is mainly allochthonous during rainy
573 seasons, e.g. soil leaching, and anthropogenic during dry seasons (industrial and
574 domestic wastewater; Dang, 2011; Le et al., 2017a). Infiltration is a key factor in the
575 hydrological pattern of this basin (Bui et al., 2014), accelerating leaching processes.
576 Soil erosion is high within the Red River basin, ranging from 1.6 to 174 t ha⁻¹ yr⁻¹ (Mai
577 et al., 2013; Nguyen et al., 2012; Podwojewski et al., 2008; Tuan et al., 2014).

578 Though the POC flux of the Red River is relatively low compared to other Asian rivers
579 (from -1% for the Yellow River to -76% for the Mekong River, Table 3), its specific yield
580 (2959 kg km⁻² yr⁻¹) is high compared to the Mekong (41%) and the Pearl River (+148%)
581 basins which are two basins close by. Le et al. (2017a) emphasised that the main
582 source of the POC was soil leaching and erosion, not phytoplankton. The soil erosion
583 in this basin is high. Besides, POC is related to SSC, and the SSC in the Thao River is
584 very high, with annual mean concentrations of 631 mg L⁻¹ at Yen Bai and 137 mg L⁻¹ at
585 Son Tay from 2003 to 2013.

586 **4.3. Controls and influences on OC fluxes**

587 Figure 9, Figure 11 and Figure 12 show the annual evolution of simulated DOC, POC
588 and TOC fluxes at four stations. The interannual variability of DOC flux is significant
589 but not massive (standard deviations equal to 14, 11, 26, and 55 kt yr⁻¹ for Yen Bai, Vu

590 Quang, Hoa Binh and Son Tay, respectively). The DOC flux was the highest in 2008
591 (Figure 9), which is the flood year and was relatively low during 2010-2013 (averagely
592 33, 49, 61 and 176 kt yr⁻¹ for Yen Bai, Vu Quang, Hoa Binh and Son Tay, respectively)
593 which are the drought years. Comparing DOC fluxes under the reference scenario
594 and current conditions allows quantifying the impacts of Q variations associated with
595 short climate variability and dam constructions (Figure 13). Under the reference
596 scenario, due to the Q variation associated with short climate variability, the DOC flux
597 during 2008-2013 only increased by 1% compared to 2003-2007, and the flood year
598 2008 was the main contributor. Under current conditions, dams induced a 13%
599 reduction of DOC flux, allowing peak flow regulation during flood seasons. Previous
600 studies also revealed that short climate variability and dam constructions within the
601 Red River basin impacted Q. However, they showed that Q was more influenced by
602 short climate variability than dams (Wei et al., 2019). They found that the annual mean
603 Q was reduced by 13% from 2000-2007 to 2008-2013 at the outlet, with 9% due to
604 short climate variability and 4% due to the dams.

605 A distinct decrease in POC flux can be noticed after 2007 at all four stations (Figure 11)
606 when some new dams started to operate. At the outlet (Son Tay), the POC flux in
607 2008 was only 45% of that in 2007, even though 2008 was a flood year, and the
608 average POC fluxes decreased by 88% in 2008-2013 compared to 2003-2007. These
609 dams have trapped the suspended sediment and changed the grain size distribution
610 of downstream sediment (Wei et al., 2019), consequently affecting the POC transfer.

611 Indeed, SSC decreased drastically by 67% in 2008 (Wei et al., 2019). Similarly to
612 DOC fluxes, POC fluxes under the reference scenario varied little (2%) between
613 2003-2007 and 2008-2013. Dams caused an 85% decrease in POC flux. Our study
614 reveals that dams induced severe sequestration of POC fluxes in the Red River basin
615 due to suspended sediment retention. This sediment retention due to damming (up to
616 90%) was already assessed in Wei et al. (2021). Reducing water and nutrient fluxes
617 might influence aquatic ecosystems and water and nutrient availability for human
618 activities in the dams and further downstream (Trinh et al., 2015).

619 Dams in this basin have different degrees of influence on DOC and POC fluxes. Our
620 conclusions are in agreement with other studies in other basins, showing that: the
621 water-sediment regulation of dams had no significant influence on DOC fluxes (Xia et
622 al., 2016a) but a substantial impact on the POC fluxes (Li et al., 2015; Xia et al.,
623 2016b).

624 Due to the drop in POC flux, the TOC flux decreased by 31% at the outlet in 2008
625 compared to the previous year (Figure 12). At Son Tay, the POC flux accounted for 74%
626 of the TOC flux during 2003-2007, while it only accounted for 47% during 2008-2013,
627 with the main part of organic carbon in the dissolved phase (Table 4). Previous studies
628 indicated that the Asian rivers draining erosion-prone mountainous terrain deliver
629 more POC than DOC, particularly during the rainy seasons (Ludwig et al., 1996; Park
630 et al., 2018). However, with the construction and operation of new dams, the
631 composition ratio of TOC changed from POC-dominating to DOC-dominating (Table

632 4). Besides, the dynamic variations of POC/TOC were also modified by dam
633 regulation (Figure 14a). Before new dam constructions, the POC/TOC ratio was low
634 around March and high in the flood season. However, after the impoundment of new
635 dams, the dams fulfilled flood-control functions during June and July, retaining water
636 and SS. Therefore, the POC/TOC ratio also decreased during the flood season.
637 Moreover, dams discharge water for irrigation around March, releasing SS, which
638 induces high POC/TOC.

639 A fundamental change in POC/TOC was observed in 2008. Two new dams (Nansha
640 on the Thao River and Tuyen Quang on the Lo River) started operation in 2008, and
641 two new dams (Madushan on the Thao River and Son La on the Da River) were
642 impounded in 2011. Compared to the other two tributaries, the POC/TOC ratio at Yen
643 Bai on the Thao River did not decrease that sharply (Table 4). The Madushan and
644 Nansha dams are around 230 km upstream of Yen Bai station. Therefore, the
645 terrestrial inputs and the river bed degradation can regulate the suspended sediment
646 and POC over this distance. At Hoa Binh station, before the new Son La dam became
647 operational, the POC/TOC percentage was already low because of the Hoa Binh dam,
648 which was impounded in 1989. Therefore, the most significant impact on the
649 POC/TOC ratio at Son Tay is due to the change of the POC/TOC from the Lo River, i.e.
650 Tuyen Quang dam contributes most to the decrease of POC/TOC at Son Tay. Dam
651 impoundments impact the hydrological cycle and nutrient cycling, which could
652 unbalance more aquatic ecosystems. Other factors related to human influence on

653 aquatic ecosystems, such as increased nutrient inputs, should be evaluated to
654 understand their impacts on OC dynamics. In the same way, modelling the full carbon
655 cycling may help identify interactions between organic and inorganic carbon within the
656 catchment (Tian et al., 2015; Nakayama, 2022). Quantifying the effects of human
657 pressures on freshwater ecosystems and the interactions between organic and
658 inorganic carbon may refine our estimates of OC exports.

659 **4.4. Errors and uncertainties in the estimation**

660 Parameters in Equations 1 and 2 were calibrated based on discrete sampling data.
661 However, sampling cannot be carried out when discharge is very high. Therefore,
662 sampling DOC and POC concentrations at high discharge were lacking. More
663 intensive sampling during flood season would help to obtain more precise parameters.
664 Some DOC sampling data can be scattered during low discharge periods due to the
665 uncertainty source, such as industrial and urban discharge. Along the Red River, the
666 inhabitants are mainly farmers and villagers who might discharge the waste into the
667 river. Moreover, %POC can vary greatly even on the same day due to the
668 instantaneous suspended sediment concentration. Hence, the data from Le et al.
669 (2017a) and Dang (2011) can differ even under a similar SSC concentration.

670 Errors in estimating OC concentration and flux can also come from the simulated Q
671 and SSC. Figure 16 presents the deviations between observed and simulated Q and
672 SSC, focusing on dates where DOC and POC sampling were conducted. It shows that
673 the POC and DOC equation parameters are determined based on a dataset not

674 representative of the different hydrological conditions, especially at Son Tay station. It
675 leads to biases, as explained in the previous paragraph.

676 Simulated Q and SSC errors are within acceptable limits (Wei et al., 2019).
677 Nevertheless, even acceptable simulated Q and SSC may lead to high biases,
678 especially at a daily time step where offsets in water or sediment transport may lead to
679 a bad representation of the peaks. Moreover, LOADEST was used to validate our
680 simulation, which can produce high biases when calculating long-term loading (Hirsch,
681 2014; Stenback et al., 2011).

682 As mentioned in section 3.1.5, POC parameters calibration was based on the data
683 sampled since 2008 when new dams started operating. Therefore, the POC
684 concentration and flux before 2008 were an insight to estimate the potential retention
685 of POC in the reservoirs roughly. According to Wei et al. (2019), the dynamic transfer
686 processes of SS before and after new dam constructions were different. Therefore,
687 POC dynamic transfer processes and fluxes would be different before and after the
688 new dam construction. Hence, the parameter b related to POC (Equation 2) should be
689 different before 2008.

690 **4.5. Perspectives**

691 In this study, we used the original version of SWAT and used simulated discharge and
692 suspended sediment fluxes combined with empirical equations to estimate organic
693 carbon loads in the Red River. We showed that a simple approach with easy-to-obtain
694 variables is limited in representing daily fluctuations of DOC and POC concentrations

695 in a watershed presenting multiple anthropogenic pressures, even if monthly
696 variations are well represented. Nevertheless, some catchment-scales models can
697 simulate carbon cycling within the watershed, including DOC and POC transport,
698 which may lead to a better representation of daily variations in DOC and POC
699 concentrations. ORCHIDEE MICT-LEAK can capture DOC dynamics and be applied
700 in large Arctic rivers (Bowring et al., 2019; 2020). In the same way, INCA-C, a revised
701 version of the INCA model, can simulate DOC fluxes in catchments (Futter et al.,
702 2007).

703 Concerning SWAT, the CENTURY model (Parton et al., 1994) was recently
704 implemented in SWAT, refining the simulation of soil organic matter dynamics (Yang et
705 al., 2016; Zhang et al., 2013; Zhang, 2018). This new version of SWAT is called
706 SWAT-C. SWAT-C was further developed by implementing modules simulating POC
707 and DOC loading and transport processes (Du et al., 2020, 2023; Qi et al., 2019,
708 2020). Applying SWAT-C on the Red River may refine the results presented in this
709 paper.

710 Moreover, a better understanding of the processes influencing OC in soils and rivers
711 and its interactions with other nutrients and a better quantification of the human
712 influence on OC transport from soils to rivers will help capture OC dynamics at the
713 outlet of watersheds under anthropogenic pressures. As an example, deeper analysis
714 on the isotopy or the stoichiometry balance of the DOC and POC within the basin may
715 help in understanding the origins of the OC transported in the Red River catchment.

716 The main contributors for POC and DOC are the Thao River and the Da River,
717 respectively. This difference in contribution may be explained by various factors such
718 as a diversity in aquatic ecosystems functioning, land use, dam management, or soil
719 type that may impact the characteristics of the organic carbon exported from the
720 tributary to the main outlet, and further its interaction with other biogeochemical cycles
721 in the delta and the sea (Luu et al., 2010).

722 **5. Conclusions**

723 Based on a hydrological model already set up, calibrated and validated over the Red
724 River basin and on DOC and POC samplings, this paper estimates DOC and POC
725 exports for ten years (2003-2013) in the large tropical Red River basin based on a
726 model of OC dynamics. Intra-annual and inter-annual variations are difficult to assess
727 from discrete in-situ samplings and only possible at the hydrometric stations. Based
728 on the daily simulated OC concentration, discharge, and suspended sediment from a
729 modelling study, daily OC fluxes were simulated considering all short-term events at
730 hydrometric stations and anywhere within the basin. It allows an understanding of the
731 spatiotemporal variations of OC in this basin.

732 Discharge and suspended sediment are crucial factors for fluvial OC fluxes. However,
733 the OC fluxes and specific yield have been altered by short climate variability and
734 intensive human activities in this basin. Especially, dam impoundments clearly
735 trapped POC, reducing TOC export and a different OC composition ratio, impacting
736 the food chain downstream.

737 This study reveals that during 2003-2013, at the outlet of the Red River basin, the
738 exports of DOC and POC were 222 and 406 kt yr⁻¹, respectively, accounting for 0.38%
739 of the total OC export by Asian rivers. However, the specific yields of DOC (1618 kg
740 km² yr⁻¹) and POC (2959 kg km² yr⁻¹) of the Red River basin were high (more than
741 double) compared to other Asian basins such as the Yellow, Yangtze, and Pearl. By
742 comparing the scenario of reference scenario (without dams) to current conditions, we
743 found a 12% and an 88% decrease in DOC and POC fluxes, respectively, mainly due
744 to dams regulations (less than 2% of variations were explained by short climate
745 variability). The percentage of POC in TOC decreased from 86% to 74% until 2007
746 and 47% with new dams. Dam constructions altered the TOC yield and its constituent
747 ratio.

748 The corresponding parameters of the DOC and POC equations well represented the
749 characteristics of each sub-basin, showing the effect of soil OC and Chlorophyll a.

750 Further research may better represent daily variations of DOC and POC
751 concentrations and the interactions with other elements to better understand the
752 anthropogenic influence on OC dynamics.

753 Finally, this study shows that climate variability may not impact OC dynamics as much
754 as damming. The latter significantly decreased POC exports due to sediment
755 retention, altering the equilibrium of OC cycling downstream, which may impact the
756 food chain. If this statement is valid for the other Asian Rivers, the quality of OC inputs
757 to the oceans may be drastically altered.

758

759 **Acknowledgement:**

760 This research was developed in the framework of the Land-Ocean-atmosphere
761 regional coupled System study center (LOTUS), an international joint
762 Vietnamese/French laboratory funded by the Institut de Recherche pour le
763 Développement (IRD). We thank LOTUS for providing the hydrological dataset, and
764 also the research travel funds for Xi Wei to collect data and information in Vietnam.
765 We also appreciate the Vietnam Academy of Science and Technology (VAST) to
766 provide organic carbon sampling data. The PhD scholarship of Xi Wei is financially
767 supported by the China Scholarship Council (CSC), grant number 201606240088.

768

769 **References:**

770 Aucour, A.-M., France-Lanord, C., Pedoja, K., Pierson-Wickmann, A.-C.,
771 Sheppard, S.M.F., 2006. Fluxes and sources of particulate organic carbon in the
772 Ganga-Brahmaputra river system: organic carbon fluxes in Ganga-Brahmaputra.
773 *Global Biogeochem. Cycles* 20, n/a-n/a. <https://doi.org/10.1029/2004GB002324>

774 Bai, Z., Feng, D., Ding, J., Duan, X., 2015. A study on the variations of soil
775 physico-chemical properties and its environmental impact factors in the Red River
776 watershed (in Chinese). *Yunnan Geogr. Environ. Res.* 27, 81–90.
777 <https://doi.org/10.13277/j.cnki.jcwu.2015.04.013>

778 Balakrishna, K., Kumar, I.A., Srinikethan, G., Mugeraya, G., 2006. Natural and
779 Anthropogenic Factors Controlling the Dissolved Organic Carbon Concentrations and
780 Fluxes in a Large Tropical River, India. *Environ Monit Assess* 122, 355–364.
781 <https://doi.org/10.1007/s10661-006-9188-7>

782 Barton, A.P., Fullen, M.A., Mitchell, D.J., Hocking, T.J., Liu, L., Wu Bo, Z., Zheng,
783 Y., Xia, Z.Y., 2004. Effects of soil conservation measures on erosion rates and crop
784 productivity on subtropical Ultisols in Yunnan Province, China. *Agriculture,
785 Ecosystems & Environment* 104, 343–357.
786 <https://doi.org/10.1016/j.agee.2004.01.034>

787 Beristain, B.T., 2005. Organic matter decomposition in simulated aquaculture
788 ponds. Wageningen University and Research.

789 Beusen, A.H.W., Dekkers, A.L.M., Bouwman, A.F., Ludwig, W., Harrison, J., 2005.
790 Estimation of global river transport of sediments and associated particulate C, N, and
791 P: River export of Particulate Matter. *Global Biogeochem. Cycles* 19, n/a-n/a.
792 <https://doi.org/10.1029/2005GB002453>

793 Bianchi, T.S., 2011. The role of terrestrially derived organic carbon in the coastal
794 ocean: A changing paradigm and the priming effect. *Proc. Natl. Acad. Sci. U.S.A.* 108,
795 19473–19481. <https://doi.org/10.1073/pnas.1017982108>

796 Boithias, L., Sauvage, S., Merlina, G., Jean, S., Probst, J.-L., Sánchez Pérez,
797 J.M., 2014. New insight into pesticide partition coefficient K_d for modelling pesticide

798 fluvial transport: Application to an agricultural catchment in south-western France.

799 Chemosphere 99, 134–142. <https://doi.org/10.1016/j.chemosphere.2013.10.050>

800 Bui, Y.T., Orange, D., Visser, S.M., Hoanh, C.T., Laissus, M., Poortinga, A., Tran,

801 D.T., Stroosnijder, L., 2013. Lumped surface and sub-surface runoff for erosion

802 modeling within a small hilly watershed in northern Vietnam: Lumped surface and

803 sub-surface runoff for erosion modeling. Hydrol. Process. n/a-n/a.

804 <https://doi.org/10.1002/hyp.9860>

805 Carlson, C.A., Hansell, D.A., 2015. Biogeochemistry of Marine Dissolved Organic

806 Matter. Elsevier. <https://doi.org/10.1016/C2012-0-02714-7>

807 Carvalhais, N., Forkel, M., Khomik, M., Bellarby, J., Jung, M., Migliavacca, M., Mu,

808 M., Saatchi, S., Santoro, M., Thurner, M., Weber, U., Ahrens, B., Beer, C., Cescatti, A.,

809 Randerson, J.T., Reichstein, M., 2014. Global covariation of carbon turnover times

810 with climate in terrestrial ecosystems. Nature 514, 213–217.

811 <https://doi.org/10.1038/nature13731>

812 Coynel, A., Seyler, P., Etcheber, H., Meybeck, M., Orange, D., 2005. Spatial and

813 seasonal dynamics of total suspended sediment and organic carbon species in the

814 Congo River: Dynamics of TSS, POC, and DOC in the Congo River. Global

815 Biogeochem. Cycles 19, n/a-n/a. <https://doi.org/10.1029/2004GB002335>

816 Dang, T. ha, 2011. Erosion et transferts de matières en suspension, carbone et

817 métaux dans le bassin versant du Fleuve Rouge depuis la frontière sino-vietnamienne

818 jusqu'à l'entrée du delta (These de doctorat). Bordeaux 1.

819 Dang, T.H., Coynel, A., Orange, D., Blanc, G., Etcheber, H., Le, L.A., 2013.
820 Seasonal Variability of Particulate Organic Carbon (POC) in a Large Asian Tropical
821 River: the Red River (China / Vietnam). *J. Sci. Technol.* 51, 315–326.
822 <https://doi.org/10.15625/0866-708X/51/3/9592>

823 Dang, T.H., Coynel, A., Orange, D., Blanc, G., Etcheber, H., Le, L.A., 2010.
824 Long-term monitoring (1960–2008) of the river-sediment transport in the Red River
825 Watershed (Vietnam): Temporal variability and dam-reservoir impact. *Science of The*
826 *Total Environment* 408, 4654–4664. <https://doi.org/10.1016/j.scitotenv.2010.07.007>

827 Ellis, E.E., Keil, R.G., Ingalls, A.E., Richey, J.E., Alin, S.R., 2012. Seasonal
828 variability in the sources of particulate organic matter of the Mekong River as
829 discerned by elemental and lignin analyses: Organic matter variability in the Mekong.
830 *J. Geophys. Res.* 117. <https://doi.org/10.1029/2011JG001816>

831 Fabre, C., Sauvage, S., Probst, J.-L., Sánchez-Pérez, J.M., 2020. Global-scale
832 daily riverine DOC fluxes from lands to the oceans with a generic model. *Global and*
833 *Planetary Change* 194, 103294. <https://doi.org/10.1016/j.gloplacha.2020.103294>

834 Fabre, C., Sauvage, S., Tananaev, N., Noël, G.E., Teisserenc, R., Probst, J.L.,
835 Pérez, J.M.S., 2019. Assessment of sediment and organic carbon exports into the
836 Arctic ocean: The case of the Yenisei River basin. *Water Research* 158, 118–135.
837 <https://doi.org/10.1016/j.watres.2019.04.018>

838 Fang, J., Tang, Y., Son, Y., 2010. Why are East Asian ecosystems important for
839 carbon cycle research? *Sci. China Life Sci.* 53, 753–756.
840 <https://doi.org/10.1007/s11427-010-4032-2>

841 Frenken, K., 2012. Irrigation in Southern and Eastern Asia in figures: AQUASTAT
842 Survey - 2011. Water Reports.

843 Galy, V., Bouchez, J., France-Lanord, C., 2007. Determination of Total Organic
844 Carbon Content and $\delta^{13}\text{C}$ in Carbonate-Rich Detrital Sediments. *Geostand
845 Geoanalyt Res* 31, 199–207. <https://doi.org/10.1111/j.1751-908X.2007.00864.x>

846 Garneau, C., 2014. Modélisation du transfert des éléments traces métalliques
847 dans les eaux de surface (These de doctorat). Toulouse 3.

848 He, D., Ren, J., Fu, K., Li, Y., 2007. Sediment change under climate changes and
849 human activities in the Yuanjiang-Red River Basin. *Chin. Sci. Bull.* 52, 164–171.
850 <https://doi.org/10.1007/s11434-007-7010-8>

851 Hirsch, R.M., 2014. Large Biases in Regression-Based Constituent Flux
852 Estimates: Causes and Diagnostic Tools. *J Am Water Resour Assoc* 50, 1401–1424.
853 <https://doi.org/10.1111/jawr.12195>

854 Hope, D., Billett, M.F., Cresser, M.S., 1994. A review of the export of carbon in
855 river water: Fluxes and processes. *Environmental Pollution* 84, 301–324.
856 [https://doi.org/10.1016/0269-7491\(94\)90142-2](https://doi.org/10.1016/0269-7491(94)90142-2)

857 Hu, B., Li, J., Bi, N., Wang, H., Wei, H., Zhao, J., Xie, L., Zou, L., Cui, R., Li, S.,

858 Liu, M., Li, G., 2015. Effect of human-controlled hydrological regime on the source,
859 transport, and flux of particulate organic carbon from the lower Huanghe (Yellow
860 River): effect of hydrological regime on particulate organic carbon. *Earth Surf.*
861 *Process. Landforms* 40, 1029–1042. <https://doi.org/10.1002/esp.3702>

862 Huang, T.-H., Fu, Y.-H., Pan, P.-Y., Chen, C.-T.A., 2012. Fluvial carbon fluxes in
863 tropical rivers. *Current Opinion in Environmental Sustainability* 4, 162–169.
864 <https://doi.org/10.1016/j.cosust.2012.02.004>

865 Huntington, T.G., Aiken, G.R., 2013. Export of dissolved organic carbon from the
866 Penobscot River basin in north-central Maine. *Journal of Hydrology* 476, 244–256.
867 <https://doi.org/10.1016/j.jhydrol.2012.10.039>

868 Le, N.D., Le, T.P.Q., Phung, T.X.B., Duong, T.T., Didier, O., 2020. Impact of
869 hydropower dam on total suspended sediment and total organic nitrogen fluxes of the
870 Red River (Vietnam). *Proc. IAHS* 383, 367–374.
871 <https://doi.org/10.5194/piahs-383-367-2020>

872 Le, T.P.Q., 2005. Biogeochemical Functioning of the Red River (North Vietnam):
873 Budgets and Modelling. The Thesis of Pierre et Marie Curie University (France).
874 Speciality: Biogeochemistry of hydrosystems PhD School: Geoscience and Natural
875 Resources.

876 Le, T.P.Q., Billen, G., Garnier, J., Théry, S., Fézard, C., Minh, C.V., 2005. Nutrient
877 (N, P) budgets for the Red River basin (Vietnam and China): Red River nutrient

878 budget. Global Biogeochem. Cycles 19, n/a-n/a.

879 <https://doi.org/10.1029/2004GB002405>

880 Le, T.P.Q., Dao, V.N., Rochelle-Newall, E., Garnier, J., Lu, X., Billen, G., Duong,

881 T.T., Ho, C.T., Etcheber, H., Nguyen, T.M.H., Nguyen, T.B.N., Nguyen, B.T., Da Le, N.,

882 Pham, Q.L., 2017a. Total organic carbon fluxes of the Red River system (Vietnam):

883 TOC fluxes of the Red River. *Earth Surf. Process. Landforms* 42, 1329–1341.

884 <https://doi.org/10.1002/esp.4107>

885 Le, T.P.Q., Garnier, J., Billen, G., Nguyen, T.M.H., Rochelle-Newall, E., Lu, X.,

886 Duong, T.T., Ho, C.T., Le, N.D., Tran, T.B.N., Marchand, C., Zhou, Y., Pham, Q.L.,

887 2017b. Riverine carbon flux from the Red River system (Viet Nam and China): a

888 modelling approach. *APN SCI BULL* 7. <https://doi.org/10.30852/sb.2017.53>

889 Le, T.P.Q., Garnier, J., Gilles, B., Sylvain, T., Van Minh, C., 2007. The changing

890 flow regime and sediment load of the Red River, Viet Nam. *Journal of Hydrology* 334,

891 199–214. <https://doi.org/10.1016/j.jhydrol.2006.10.020>

892 Le, T.P.Q., Le, N.D., Dao, V.N., Rochelle-Newall, E., Nguyen, T.M.H., Marchand,

893 C., Duong, T.T., Phung, T.X.B., 2018. Change in carbon flux (1960–2015) of the Red

894 River (Vietnam). *Environ Earth Sci* 77, 658.

895 <https://doi.org/10.1007/s12665-018-7851-2>

896 Li, G., Wang, X.T., Yang, Z., Mao, C., West, A.J., Ji, J., 2015. Dam-triggered

897 organic carbon sequestration makes the Changjiang (Yangtze) river basin (China) a

898 significant carbon sink. *J. Geophys. Res. Biogeosci.* 120, 39–53.
899 <https://doi.org/10.1002/2014JG002646>

900 Li, M., Peng, C., Wang, M., Xue, W., Zhang, K., Wang, K., Shi, G., Zhu, Q., 2017.
901 The carbon flux of global rivers: A re-evaluation of amount and spatial patterns.
902 *Ecological Indicators* 80, 40–51. <https://doi.org/10.1016/j.ecolind.2017.04.049>

903 Li, M., Peng, C., Zhou, X., Yang, Y., Guo, Y., Shi, G., Zhu, Q., 2019. Modeling
904 Global Riverine DOC Flux Dynamics From 1951 to 2015. *J. Adv. Model. Earth Syst.*
905 11, 514–530. <https://doi.org/10.1029/2018MS001363>

906 Li, S., Lu, X.X., Bush, R.T., 2013. CO₂ partial pressure and CO₂ emission in the
907 Lower Mekong River. *Journal of Hydrology* 504, 40–56.
908 <https://doi.org/10.1016/j.jhydrol.2013.09.024>

909 Li, X., Li, Y., He, J., Luo, X., 2016. Analysis of variation in runoff and impacts
910 factors in the Yuanjiang-Red River Basin from 1956 to 2013. *Resour. Sci.* 38,
911 1149–1159. <https://doi.org/10.18402/resci.2016.06.14>

912 Li, Y., He, D., Ye, C., 2008. Spatial and temporal variation of runoff of Red River
913 Basin in Yunnan. *J. Geogr. Sci.* 18, 308–318.
914 <https://doi.org/10.1007/s11442-008-0308-x>

915 Li, Y., Hu, J., Han, X., Li, Yuxiang, Li, Yawen, He, B., Duan, X., 2019. Effects of
916 past land use on soil organic carbon changes after dam construction. *Science of The*
917 *Total Environment* 686, 838–846. <https://doi.org/10.1016/j.scitotenv.2019.06.030>

918 Lloret, E., Dessert, C., Buss, H.L., Chaduteau, C., Huon, S., Alberic, P., Benedetti,
919 M.F., 2016. Sources of dissolved organic carbon in small volcanic mountainous
920 tropical rivers, examples from Guadeloupe (French West Indies). *Geoderma* 282,
921 129–138. <https://doi.org/10.1016/j.geoderma.2016.07.014>

922 Lu, X.X., Oeurng, C., Le, T.P.Q., Thuy, D.T., 2015. Sediment budget as affected
923 by construction of a sequence of dams in the lower Red River, Viet Nam.
924 *Geomorphology* 248, 125–133. <https://doi.org/10.1016/j.geomorph.2015.06.044>

925 Ludwig, W., Probst, J.-L., Kempe, S., 1996. Predicting the oceanic input of
926 organic carbon by continental erosion. *Global Biogeochem. Cycles* 10, 23–41.
927 <https://doi.org/10.1029/95GB02925>

928 Luu, T.N.M., Garnier, J., Billen, G., Le, T.P.Q., Nemery, J., Orange, D., Le, L.A.,
929 2012. N, P, Si budgets for the Red River Delta (northern Vietnam): how the delta
930 affects river nutrient delivery to the sea. *Biogeochemistry* 107, 241–259.
931 <https://doi.org/10.1007/s10533-010-9549-8>

932 Luu, T.N.M., Garnier, J., Billen, G., Orange, D., Némery, J., Le, T.P.Q., Tran, H.T.,
933 Le, L.A., 2010. Hydrological regime and water budget of the Red River Delta
934 (Northern Vietnam). *Journal of Asian Earth Sciences* 37, 219–228.
935 <https://doi.org/10.1016/j.jseaes.2009.08.004>

936 Mai, V.T., van Keulen, H., Hessel, R., Ritsema, C., Roetter, R., Phien, T., 2013.
937 Influence of paddy rice terraces on soil erosion of a small watershed in a hilly area of

938 Northern Vietnam. Paddy Water Environ 11, 285–298.
939 <https://doi.org/10.1007/s10333-012-0318-2>

940 Manninen, N., Soenne, H., Lemola, R., Hoikkala, L., Turtola, E., 2018. Effects of
941 agricultural land use on dissolved organic carbon and nitrogen in surface runoff and
942 subsurface drainage. Science of The Total Environment 618, 1519–1528.
943 <https://doi.org/10.1016/j.scitotenv.2017.09.319>

944 McClelland, J.W., Stieglitz, M., Pan, F., Holmes, R.M., Peterson, B.J., 2007.
945 Recent changes in nitrate and dissolved organic carbon export from the upper
946 Kuparuk River, North Slope, Alaska: N and C export from the Kuparuk River. J.
947 Geophys. Res. 112, n/a-n/a. <https://doi.org/10.1029/2006JG000371>

948 Moreira-Turcq, P., Seyler, P., Guyot, J.L., Etcheber, H., 2003. Exportation of
949 organic carbon from the Amazon River and its main tributaries. Hydrol. Process. 17,
950 1329–1344. <https://doi.org/10.1002/hyp.1287>

951 Moriasi, D.N., Arnold, J.G., Liew, M.W.V., Bingner, R.L., Harmel, R.D., Veith, T.L.,
952 2007. Model Evaluation Guidelines for Systematic Quantification of Accuracy in
953 Watershed Simulations. Transactions of the ASABE 50, 885–900.
954 <https://doi.org/10.13031/2013.23153>

955 Nash, J.E., Sutcliffe, J.V., 1970. River flow forecasting through conceptual models
956 part I — A discussion of principles. Journal of Hydrology 10, 282–290.
957 [https://doi.org/10.1016/0022-1694\(70\)90255-6](https://doi.org/10.1016/0022-1694(70)90255-6)

958 Neitsch, S.L., Arnold, J.G., Kiniry, J.R., Williams, J.R., 2011. Soil and water
959 assessment tool theoretical documentation version 2009. Texas Water Resources
960 Institute.

961 Nguyen, H.T.M., Billen, G., Garnier, J., Le, T.P.Q., Pham, Q.L., Huon, S.,
962 Rochelle-Newall, E., 2018. Organic carbon transfers in the subtropical Red River
963 system (Viet Nam): insights on CO₂ sources and sinks. *Biogeochemistry* 138,
964 277–295. <https://doi.org/10.1007/s10533-018-0446-x>

965 Nguyen, V.T., Orange, D., Laffly, D., Pham, V.Q., 2012. Consequences of large
966 hydropower dams on erosion budget within hilly agricultural catchments in Northern
967 Vietnam by RUSLE modeling, in: *Proceedings of the International Conference*
968 *Sediment Transport Modeling in Hydrological Watersheds and Rivers*, Istanbul,
969 Turkey, pp. 14–16.

970 Ni, H.-G., Lu, F.-H., Luo, X.-L., Tian, H.-Y., Zeng, E.Y., 2008. Riverine inputs of
971 total organic carbon and suspended particulate matter from the Pearl River Delta to
972 the coastal ocean off South China. *Marine Pollution Bulletin* 56, 1150–1157.
973 <https://doi.org/10.1016/j.marpolbul.2008.02.030>

974 Park, J.-H., Nayna, O.K., Begum, M.S., Chea, E., Hartmann, J., Keil, R.G., Kumar,
975 S., Lu, X., Ran, L., Richey, J.E., Sarma, V.V.S.S., Tareq, S.M., Xuan, D.T., Yu, R.,
976 2018. Reviews and syntheses: Anthropogenic perturbations to carbon fluxes in Asian
977 river systems – concepts, emerging trends, and research challenges. *Biogeosciences*
978 15, 3049–3069. <https://doi.org/10.5194/bg-15-3049-2018>

979 Podwojewski, P., Orange, D., Jouquet, P., Valentin, C., Nguyen, V.T., Janeau, J.L.,
980 Tran, D.T., 2008. Land-use impacts on surface runoff and soil detachment within
981 agricultural sloping lands in Northern Vietnam. *CATENA* 74, 109–118.
982 <https://doi.org/10.1016/j.catena.2008.03.013>

983 Ran, L., Lu, X.X., Sun, H., Han, J., Li, R., Zhang, J., 2013. Spatial and seasonal
984 variability of organic carbon transport in the Yellow River, China. *Journal of Hydrology*
985 498, 76–88. <https://doi.org/10.1016/j.jhydrol.2013.06.018>

986 Rizinjirabake, F., Abdi, A.M., Tenenbaum, D.E., Pilesjö, P., 2018. Riverine
987 dissolved organic carbon in Rukarara River Watershed, Rwanda. *Science of The Total*
988 *Environment* 643, 793–806. <https://doi.org/10.1016/j.scitotenv.2018.06.194>

989 Rousseau, J.-F., 2015. Green energies the socialist way: hydropower, energy
990 crops and Handai livelihoods along the Red river, Yunnan province, China. McGill
991 University (Canada).

992 Runkel, R.L., Crawford, C.G., Cohn, T.A., 2004. Load Estimator (LOADEST): A
993 FORTRAN program for estimating constituent loads in streams and rivers.

994 Seitzinger, S.P., Mayorga, E., Bouwman, A.F., Kroeze, C., Beusen, A.H.W., Billen,
995 G., Van Drecht, G., Dumont, E., Fekete, B.M., Garnier, J., Harrison, J.A., 2010. Global
996 river nutrient export: A scenario analysis of past and future trends: Global river export
997 scenarios. *Global Biogeochem. Cycles* 24, n/a-n/a.
998 <https://doi.org/10.1029/2009GB003587>

999 Shi, S., Yang, M., Hou, Y., Peng, C., Wu, H., Zhu, Q., Liang, Q., Xie, J., Wang, M.,
1000 2019. Simulation of dissolved organic carbon concentrations and fluxes in Chinese
1001 monsoon forest ecosystems using a modified TRIPLEX-DOC model. *Science of The*
1002 *Total Environment* 697, 134054. <https://doi.org/10.1016/j.scitotenv.2019.134054>

1003 Sickman, J.O., Zanolli, M.J., Mann, H.L., 2007. Effects of Urbanization on Organic
1004 Carbon Loads in the Sacramento River, California: Urbanization and riverine carbon
1005 loads. *Water Resour. Res.* 43. <https://doi.org/10.1029/2007WR005954>

1006 Spencer, R.G.M., Hernes, P.J., Dinga, B., Wabakanghanzi, J.N., Drake, T.W., Six,
1007 J., 2016. Origins, seasonality, and fluxes of organic matter in the Congo River:
1008 Organic Matter in the Congo River. *Global Biogeochem. Cycles* 30, 1105–1121.
1009 <https://doi.org/10.1002/2016GB005427>

1010 Stenback, G.A., Crumpton, W.G., Schilling, K.E., Helmers, M.J., 2011. Rating
1011 curve estimation of nutrient loads in Iowa rivers. *Journal of Hydrology* 396, 158–169.
1012 <https://doi.org/10.1016/j.jhydrol.2010.11.006>

1013 Tamm, T., Nõges, T., Järvet, A., Bouraoui, F., 2008. Contributions of DOC from
1014 surface and groundflow into Lake Võrtsjärv (Estonia). *Hydrobiologia* 599, 213–220.
1015 <https://doi.org/10.1007/s10750-007-9189-8>

1016 Trinh, D.A., Luu, T.N.M., Trinh, Q.H., Tran, H.S., Tran, T.M., Le, T.P.Q., Duong,
1017 T.T., Orange, D., Janeau, J.L., Pommier, T., Rochelle-Newall, E., 2016. Impact of
1018 terrestrial runoff on organic matter, trophic state, and phytoplankton in a tropical,

1019 upland reservoir. *Aquat Sci* 78, 367–379. <https://doi.org/10.1007/s00027-015-0439-y>

1020 Tuan, V.D., Hilger, T., MacDonald, L., Clemens, G., Shiraishi, E., Vien, T.D., Stahr,
1021 K., Cadisch, G., 2014. Mitigation potential of soil conservation in maize cropping on
1022 steep slopes. *Field Crops Research* 156, 91–102.
1023 <https://doi.org/10.1016/j.fcr.2013.11.002>

1024 Vinh, V.D., Ouillon, S., Thanh, T.D., Chu, L.V., 2014. Impact of the Hoa Binh dam
1025 (Vietnam) on water and sediment budgets in the Red River basin and delta. *Hydrol.*
1026 *Earth Syst. Sci.* 18, 3987–4005. <https://doi.org/10.5194/hess-18-3987-2014>

1027 Vörösmarty, C., Meybeck, M., Fekete, B., Sharma, K., 1997. The potential impact
1028 of neo-Castorization on sediment transport by the global network of rivers. *Hum.*
1029 *Impact Eros. Sediment* 245, 261–273.

1030 Wang, H., Saito, Y., Zhang, Y., Bi, N., Sun, X., Yang, Z., 2011. Recent changes of
1031 sediment flux to the western Pacific Ocean from major rivers in East and Southeast
1032 Asia. *Earth-Science Reviews* 108, 80–100.
1033 <https://doi.org/10.1016/j.earscirev.2011.06.003>

1034 Wang, X., Ma, H., Li, R., Song, Z., Wu, J., 2012. Seasonal fluxes and source
1035 variation of organic carbon transported by two major Chinese Rivers: The Yellow
1036 River and Changjiang (Yangtze) River: FLUX AND SOURCE OF ORGANIC CARBON.
1037 *Global Biogeochem. Cycles* 26, n/a-n/a. <https://doi.org/10.1029/2011GB004130>

1038 Wei, X., Sauvage, S., Le, T.P.Q., Ouillon, S., Orange, D., Vinh, V.D.,

1039 Sanchez-Perez, J.-M., 2019. A Modeling Approach to Diagnose the Impacts of Global
1040 Changes on Discharge and Suspended Sediment Concentration within the Red River
1041 Basin. *Water* 11, 958. <https://doi.org/10.3390/w11050958>

1042 Wei, X., Sauvage, S., Ouillon, S., Le, T.P.Q., Orange, D., Herrmann, M.,
1043 Sanchez-Perez, J.-M., 2021. A modelling-based assessment of suspended sediment
1044 transport related to new damming in the Red River basin from 2000 to 2013. *CATENA*
1045 197, 104958. <https://doi.org/10.1016/j.catena.2020.104958>

1046 Wen, H., Perdrial, J., Bernal, S., Abbott, B.W., Dupas, R., Godsey, S.E., Harpold,
1047 A., Rizzo, D., Underwood, K., Adler, T., Hale, R., Sterle, G., Li, L., 2019. Temperature
1048 controls production but hydrology controls export of dissolved organic carbon at the
1049 catchment scale (preprint). *Biogeochemical processes/Theory development*.
1050 <https://doi.org/10.5194/hess-2019-310>

1051 Xia, X., Dong, J., Wang, M., Xie, H., Xia, N., Li, H., Zhang, X., Mou, X., Wen, J.,
1052 Bao, Y., 2016a. Effect of water-sediment regulation of the Xiaolangdi reservoir on the
1053 concentrations, characteristics, and fluxes of suspended sediment and organic carbon
1054 in the Yellow River. *Science of The Total Environment* 571, 487–497.
1055 <https://doi.org/10.1016/j.scitotenv.2016.07.015>

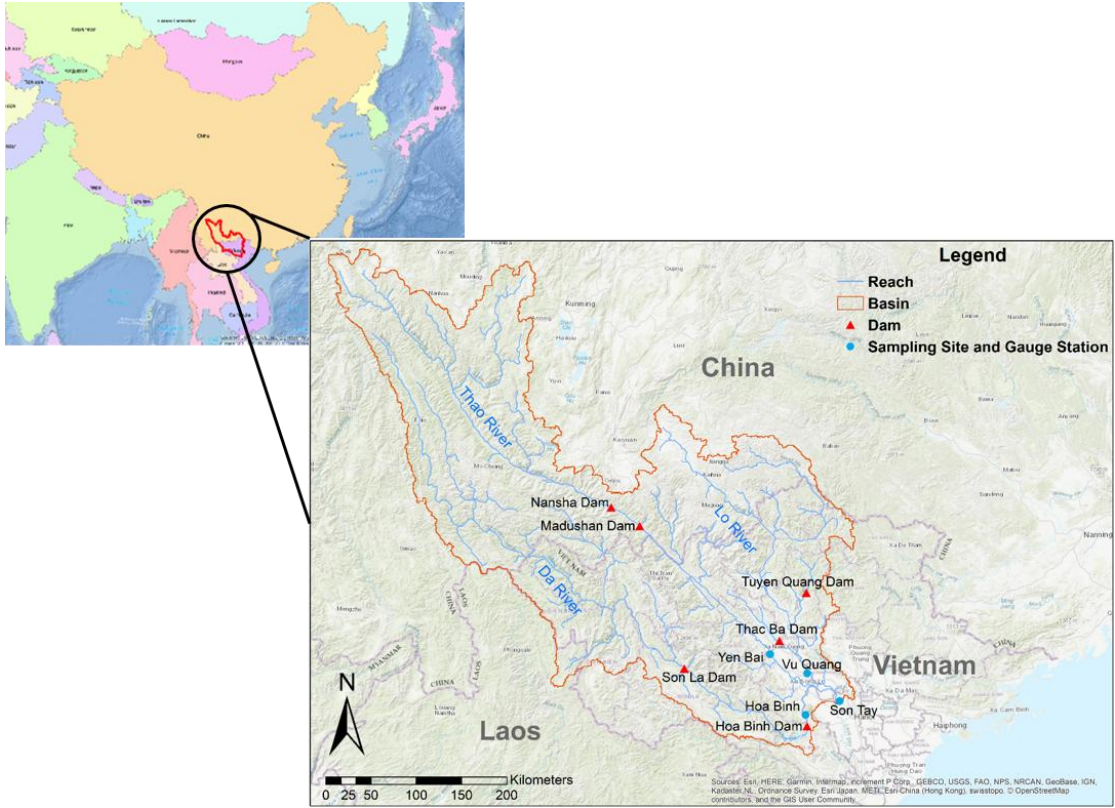
1056 Xia, X., Dong, J., Wang, M., Xie, H., Xia, N., Li, H., Zhang, X., Mou, X., Wen, J.,
1057 Bao, Y., 2016b. Effect of water-sediment regulation of the Xiaolangdi reservoir on the
1058 concentrations, characteristics, and fluxes of suspended sediment and organic carbon
1059 in the Yellow River. *Science of The Total Environment* 571, 487–497.

1060 <https://doi.org/10.1016/j.scitotenv.2016.07.015>

1061 Xie, S., 2002. The Hydrological Characteristics of the Red River Basin. *Hydrol.* 22,
1062 53–63. <https://doi.org/10.3969/j.issn.1000-0852.2002.04.017>

1063 Zarfl, C., Lumsdon, A.E., Berlekamp, J., Tydecks, L., Tockner, K., 2015. A global
1064 boom in hydropower dam construction. *Aquat Sci* 77, 161–170.
1065 <https://doi.org/10.1007/s00027-014-0377-0>

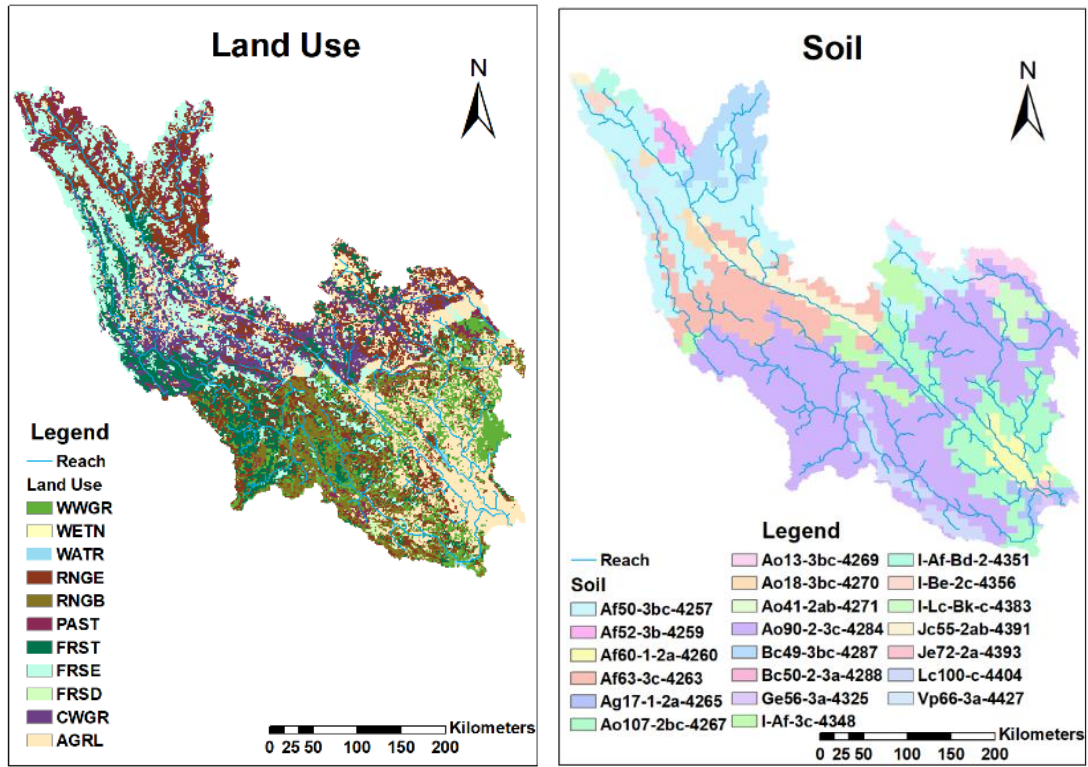
1066



1067

1068 Figure 1. The Red River watershed (red outline), with its three main tributaries (the Thao River, the Da
 1069 River and the Lo River); sampling sites and gauge stations (blue points); large dams locations (red
 1070 triangles).

1071

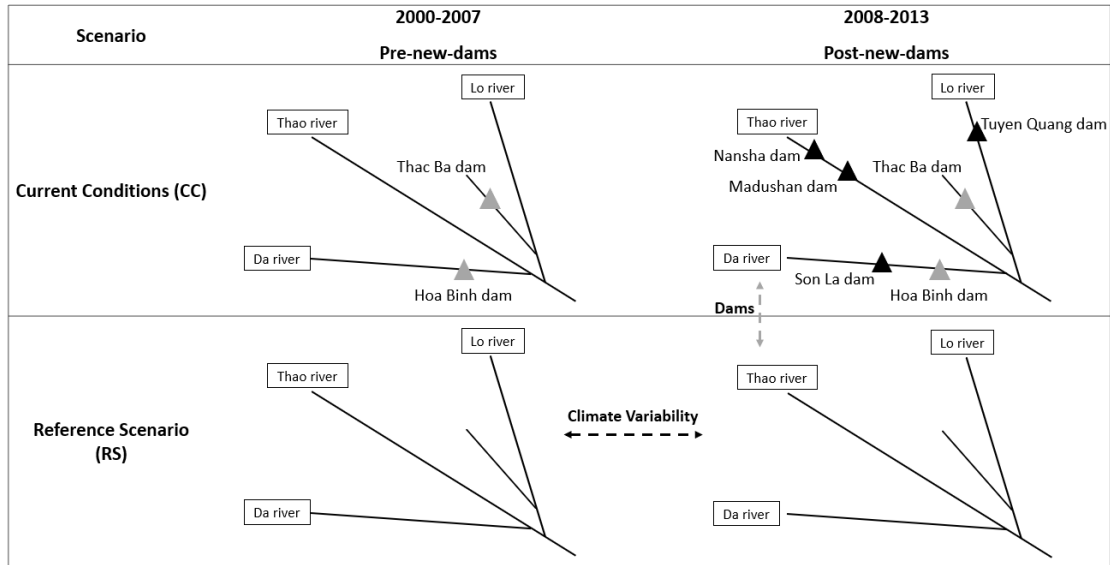


1072

1073

Figure 2. Land use and soil map of the Red River basin (Wei et al., 2019).

1074



1075

1076

1077

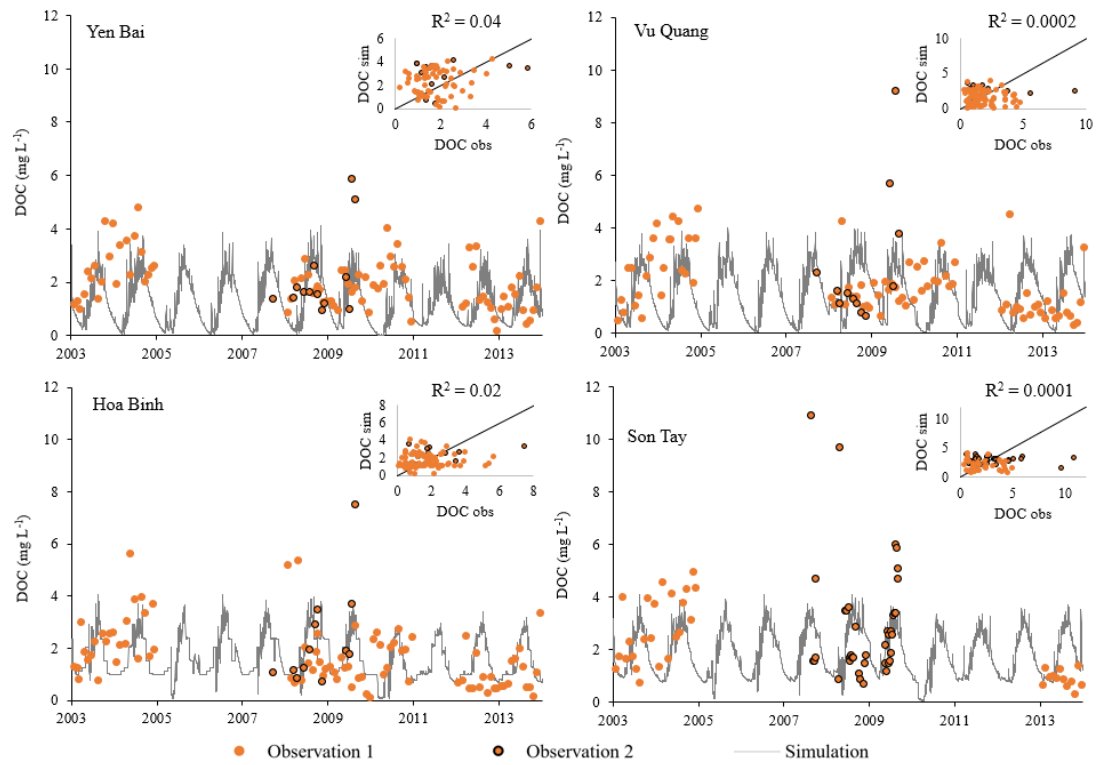
1078

1079

1080

1081

Figure 3. The setting for Current Conditions and Reference Scenario: grey triangles are the old dams impounded before the study period, and black triangles are the new dams impounded since 2008. By comparing current conditions to the reference scenario during 2008-2013, the impacts of these dams can be quantified; by comparing the period 2008-2013 to 2003-2007 under the reference scenario, the impacts of short climate variability can be quantified.

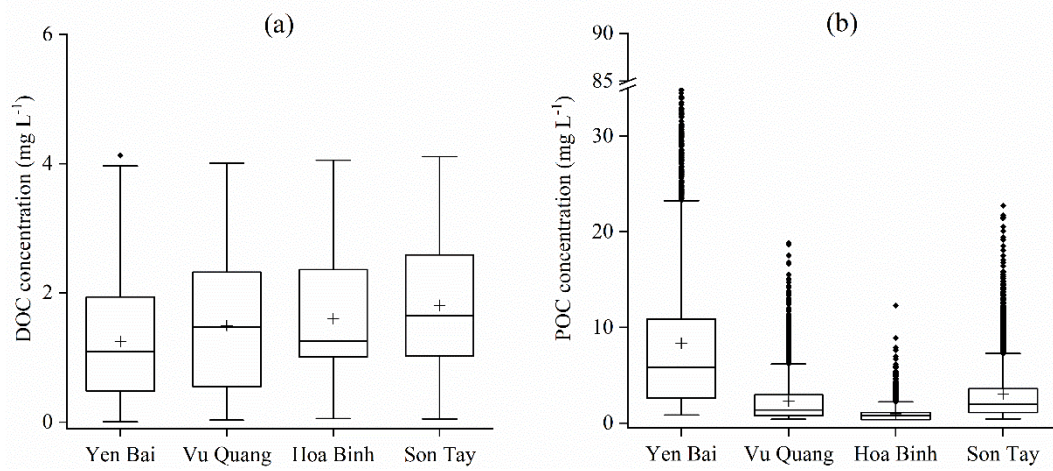


1082

1083 Figure 4. Daily variations of dissolved organic carbon (DOC) concentration (mg L^{-1}) at four stations from
 1084 2003 to 2013. Observation 1 (orange dots) shows the DOC measured by Le et al. (2017a); observation 2
 1085 (orange and black dots) indicates the DOC measured by Dang (2006); calculations from Equation 1 based
 1086 on the simulated discharge ($Q, \text{m}^3 \text{s}^{-1}$) from Wei et al. (2019) with the values of the parameters given in
 1087 Table 1 are the solid grey line.

1088

25%~75%
 Range within 1.5IQR
 Median Line
+ Mean
• Outliers

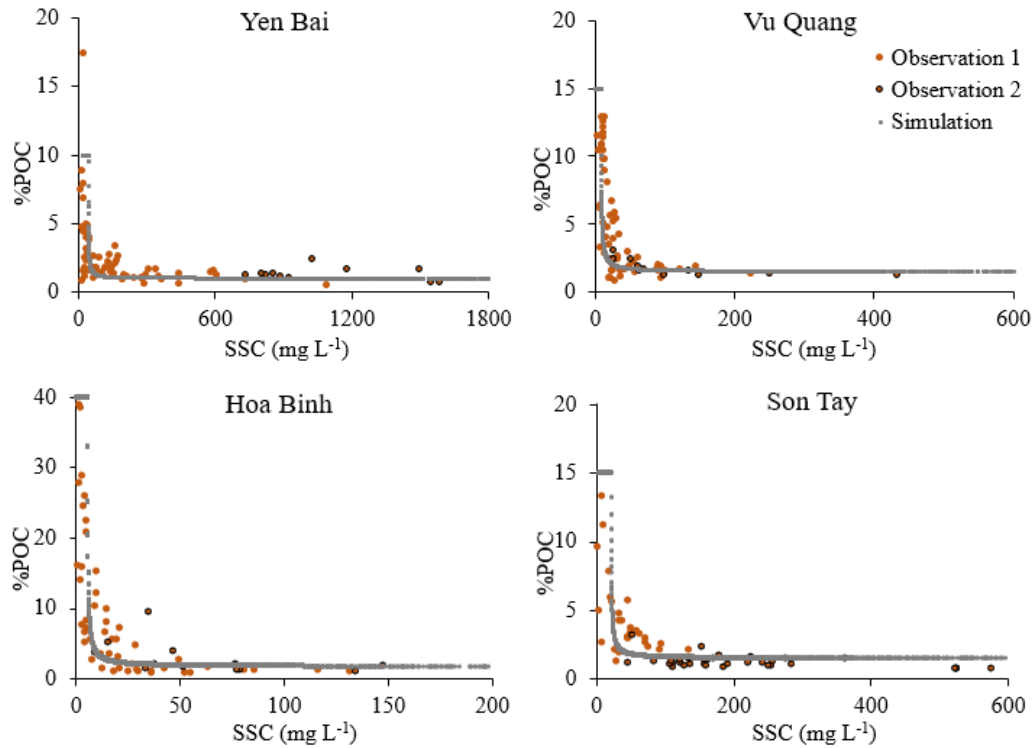


1089

1090 Figure 5. Box plot of daily simulated dissolved organic carbon (DOC) and daily particulate organic carbon
 1091 (POC) concentration (mg L⁻¹) at four stations during 2003-2013 in the Red River basin. IQR represents the
 1092 interquartile range.

1093

1094

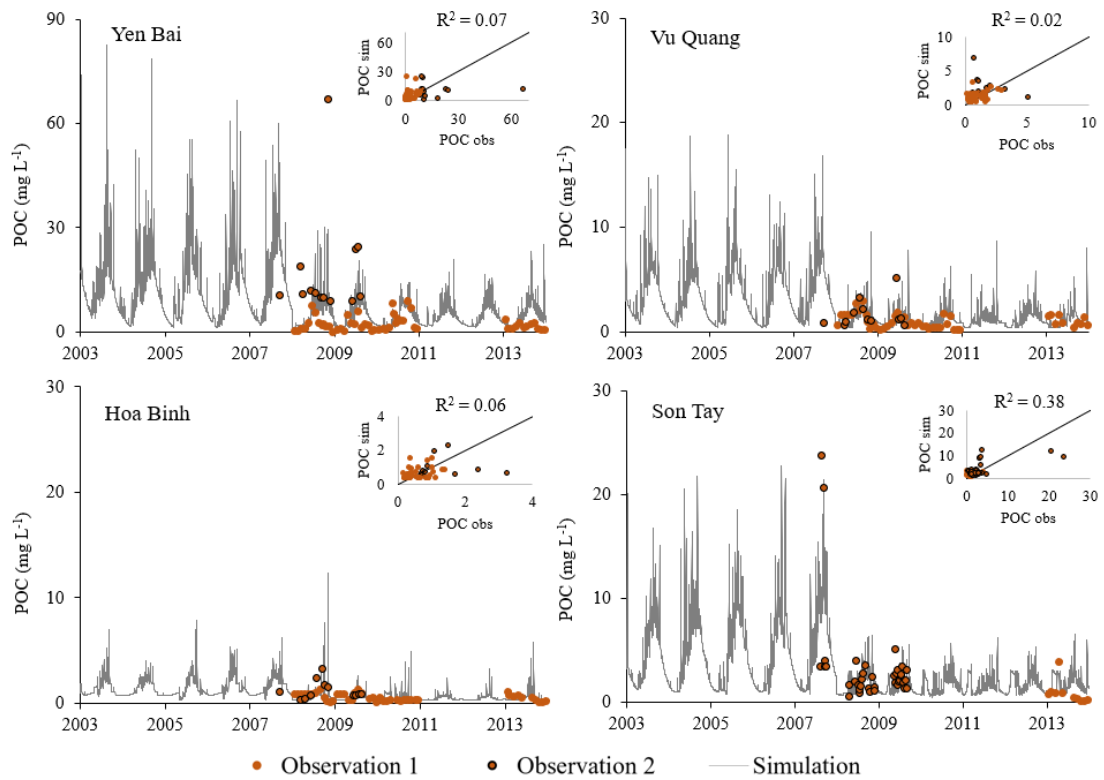


1095

1096 Figure 6. Relationship between the percentage of POC concentration (%POC) in the suspended sediment
 1097 concentration (SSC, mg L^{-1}) and observed SSC (mg L^{-1}). Observation 1 (black dot) corresponds to the
 1098 measurements from Le et al. (2017a); observation 2 (black and brown dots) corresponds to the
 1099 measurements from Dang (2006); brown dots were the calculations from Equation 2 based on the
 1100 observed SSC data collected from the Vietnam Ministry of Natural Resources and Environment
 1101 (MONRE). $\%POC_{\text{max}}$, the maximum limit of %POC, was set as 10%, 15%, 40% and 15% for Yen Bai, Vu
 1102 Quang, Hoa Binh and Son Tay, respectively.

1103

1104

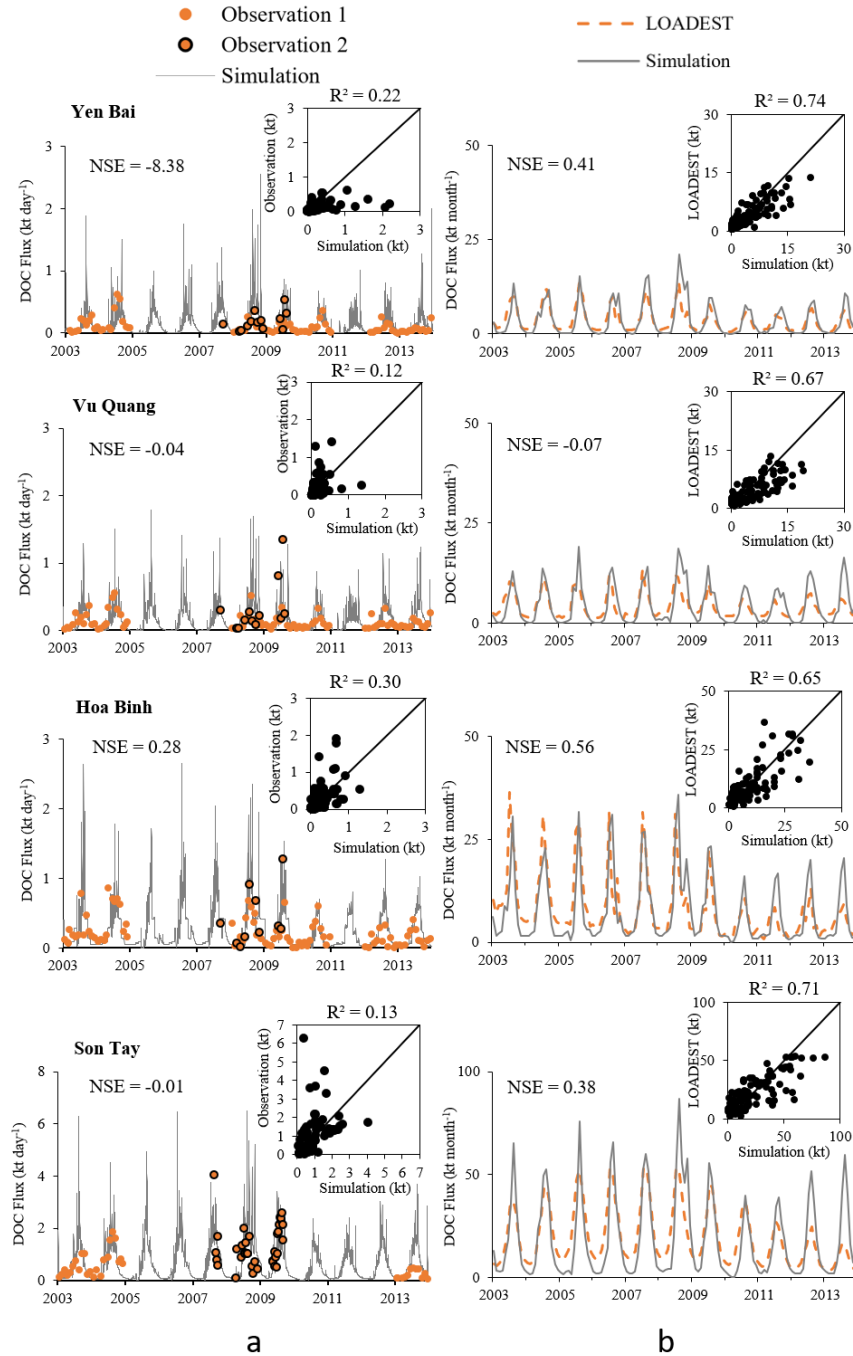


1105

1106 Figure 7. Daily variation of particulate organic carbon (POC) concentration (mg L^{-1}) at four stations from
 1107 2003 to 2013. Observation 1 (brown dots) was observed POC from Le et al. (2017a); observation 2 (brown and black dots)
 1108 was the observed POC from Dang (2006); simulation (solid grey line) was calculated from
 1109 Equation 2 based on the simulated suspended sediment concentration (SSC , mg L^{-1}) from Wei et al.
 1110 (2019).

1111

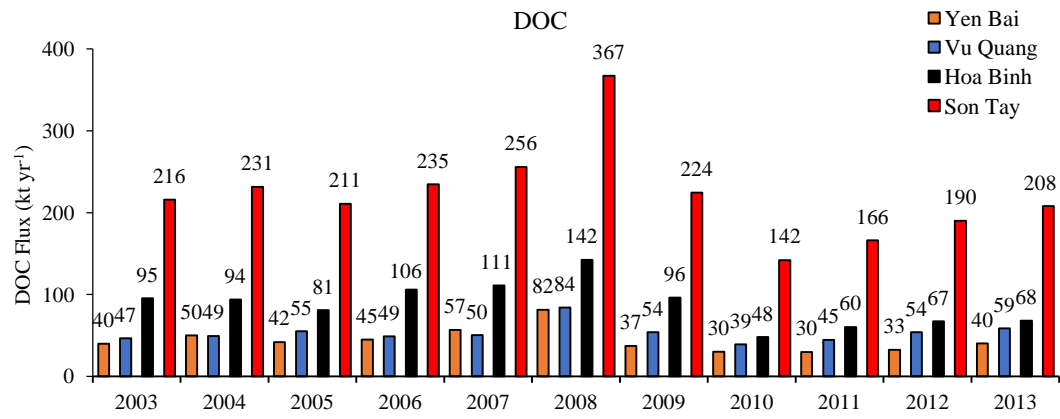
1112



1113

1114 Figure 8. (a) Mean daily variation of dissolved organic carbon (DOC) fluxes (kt day⁻¹) at four stations from
 1115 2003 to 2013. Observation 1 (orange dots) was calculated from the measured DOC concentration from Le
 1116 et al. (2017a); observation 2 (orange and black dots) was calculated from the measured DOC
 1117 concentration from Dang (2006); the solid grey line was the simulated DOC fluxes (kt day⁻¹) calculated
 1118 based on the DOC concentrations from Equation 1 and the Q from SWAT model. (b) Mean monthly DOC
 1119 fluxes (kt month⁻¹) comparison between results from LOADEST and our calculations.

1120

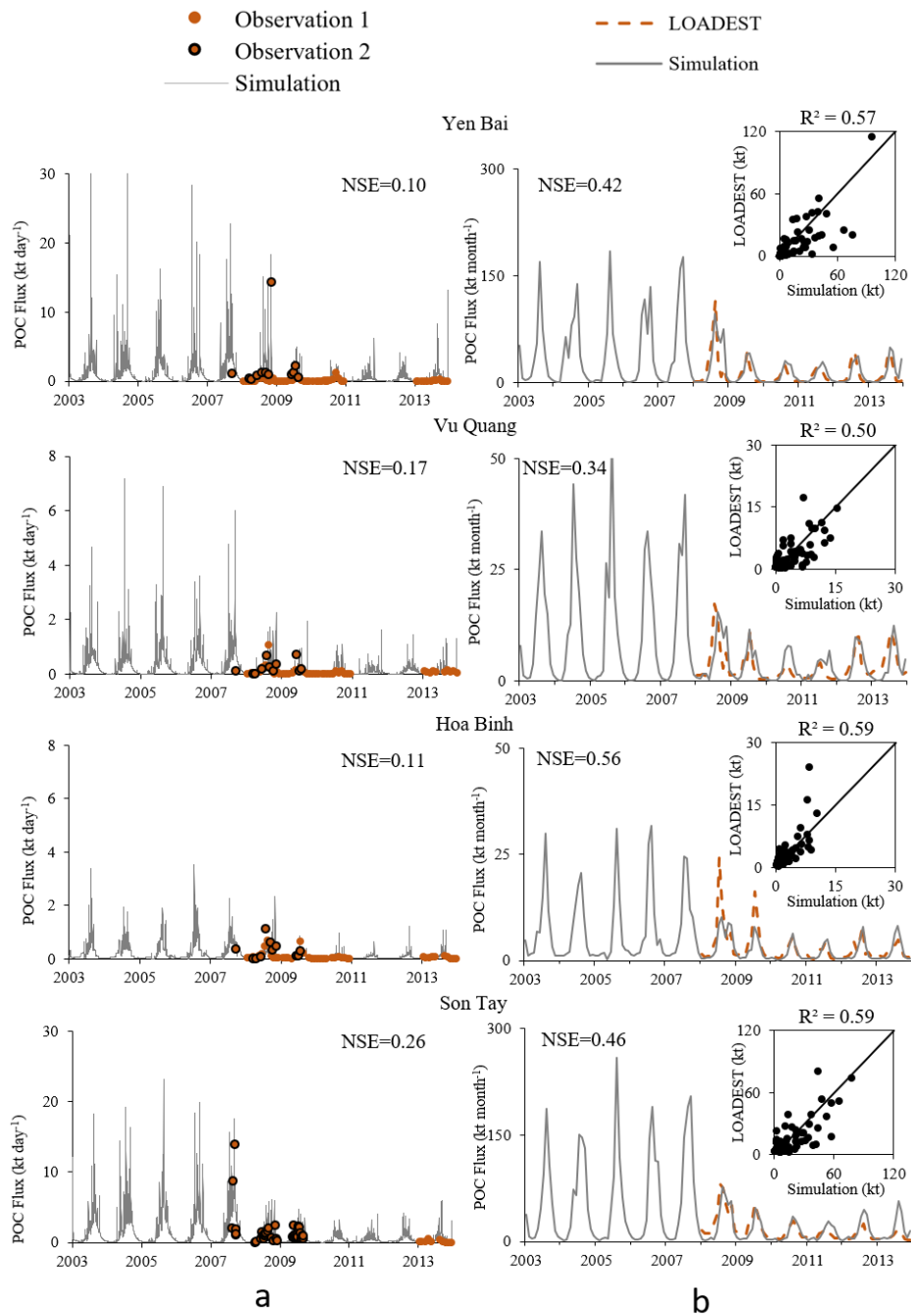


1121

1122 Figure 9. Simulated annual dissolved organic carbon (DOC) fluxes (kt yr^{-1}) at four stations from 2003 to
 1123 2013.

1124

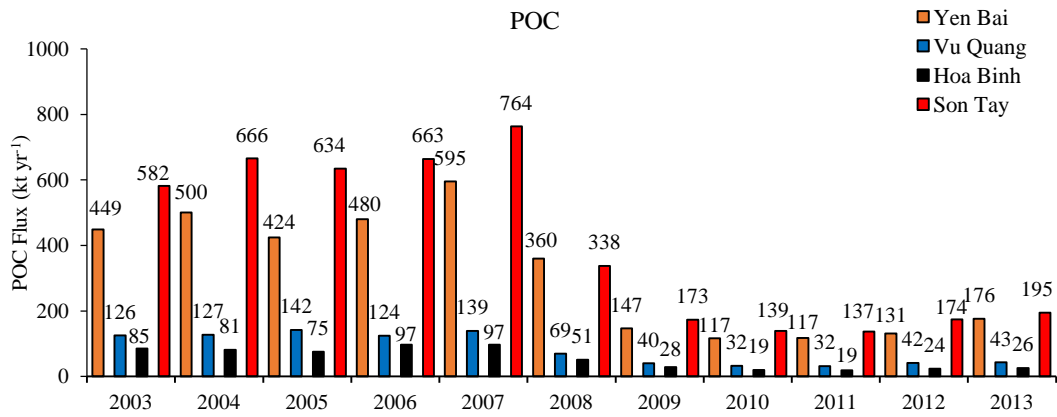
1125



1126

1127 Figure 10. (a) Mean daily variation of particulate organic carbon (POC) flux (kt day^{-1}) at four stations from
 1128 2003 to 2013. Observation 1 (brown dots) was calculated from the measured POC concentration from Le
 1129 et al. (2017a); observation 2 (brown and black dots) was calculated from the measured POC
 1130 concentration from Dang (2006); the solid gray line was the simulated POC flux (kt day^{-1}) based on the
 1131 POC concentrations from Equation 2 and the Q from SWAT model. (b) Mean monthly POC flux (kt month^{-1})
 1132 comparison between LOADEST results and our calculations during 2008-2013.

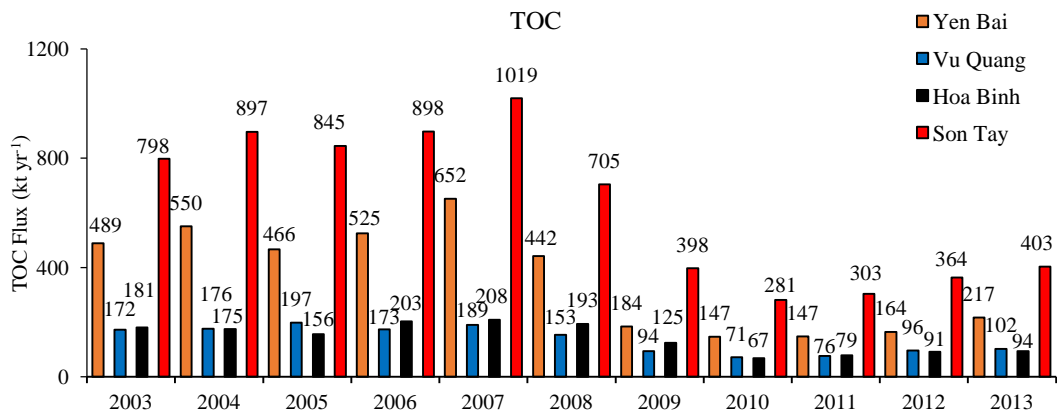
1133



1134

1135 Figure 112. Simulated annual particulate organic carbon (POC) fluxes (kt yr⁻¹) at four stations from 2003 to
1136 2013.

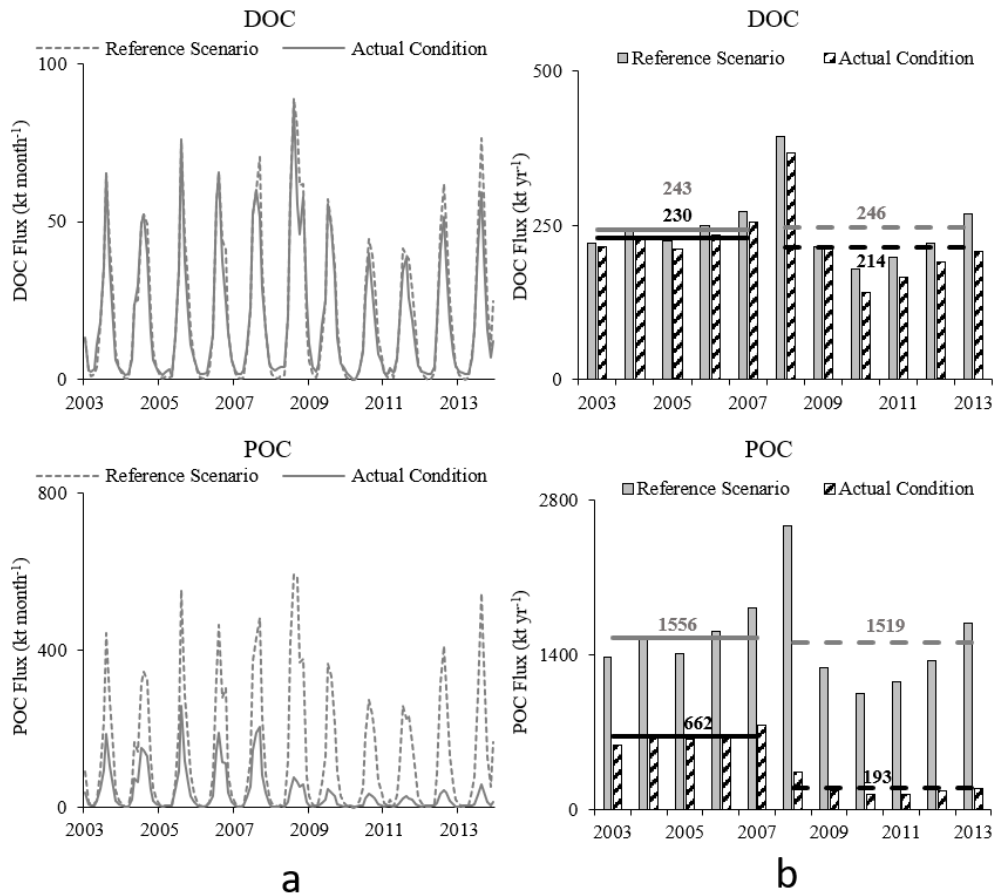
1137



1138

1139 Figure 12. Simulated annual total organic carbon (TOC) flux (kt yr⁻¹) at four stations from 2003 to 2013.

1140

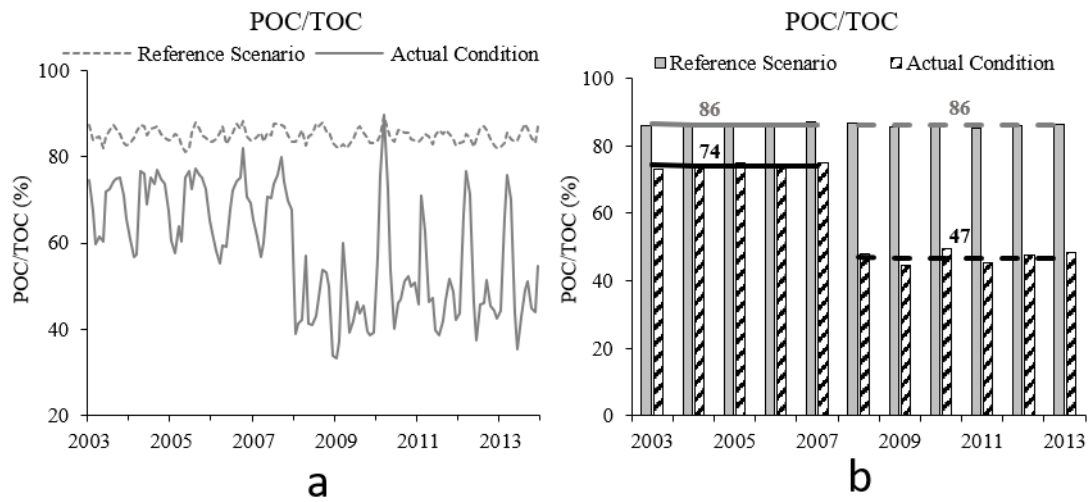


1141

1142 Figure 13. Simulated dissolved organic carbon (DOC) and particulate organic carbon (POC) fluxes at Son
 1143 Tay station under reference scenario and current conditions: (a) Monthly variations; (b) Annual budgets.
 1144 The solid black line displays the total decrease caused by short climate variability and dams between
 1145 2003-2007 and 2008-2013; the grey dashed line indicates the decrease related to short climate variability,
 1146 and the black dashed line displays the reduction caused by dams.

1147

1148

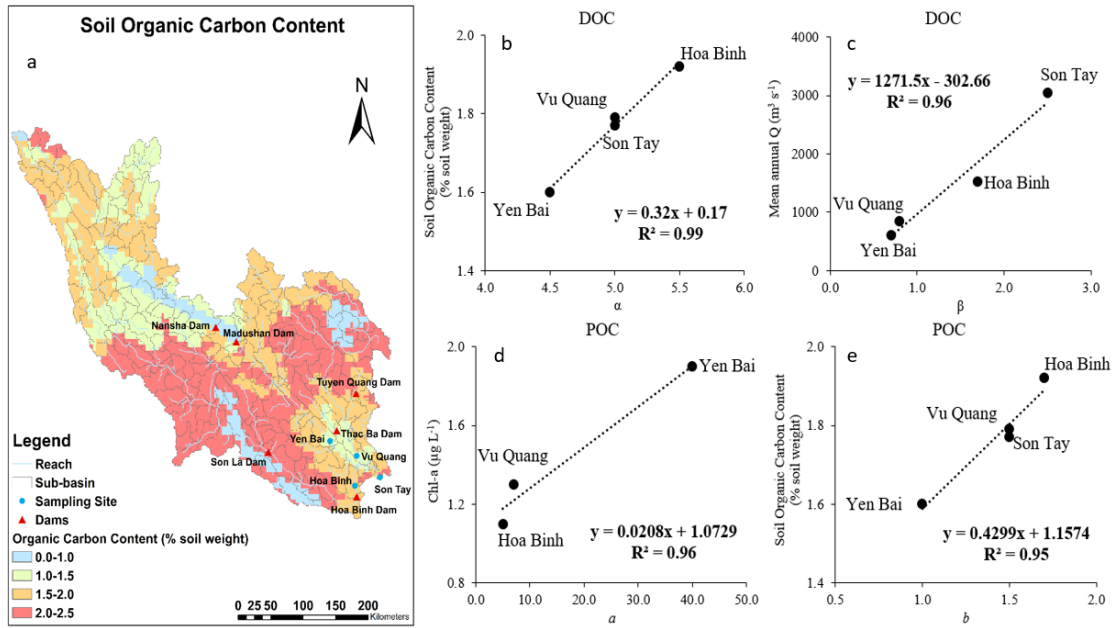


1149

1150 Figure 14. Simulated particulate organic carbon (POC) percentage in total organic carbon (TOC) during
 1151 2003-2013 under reference scenario and current conditions: (a) mean monthly variations; (b) mean
 1152 annual values.

1153

1154

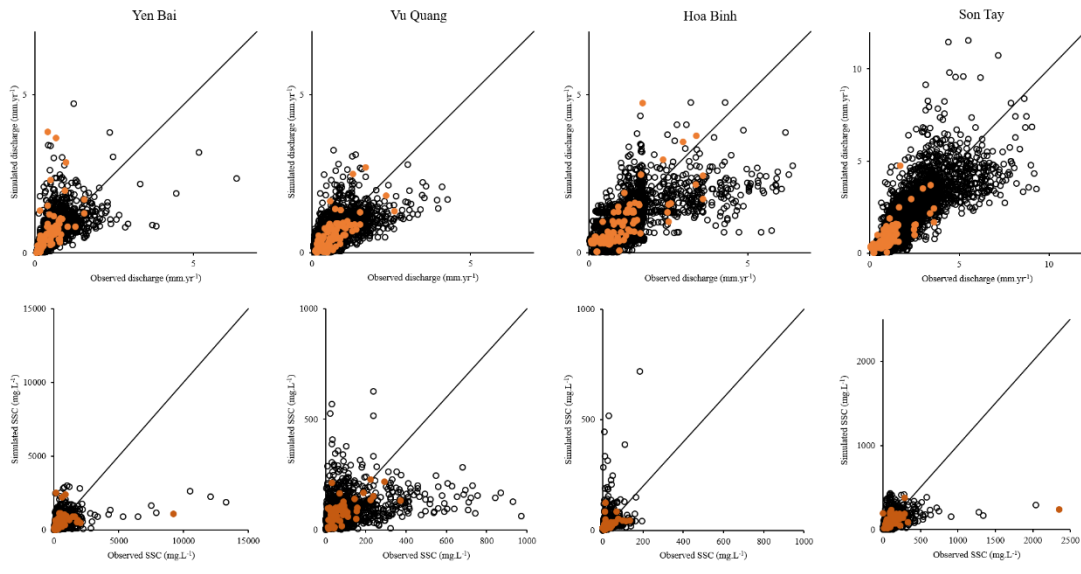


1155

1156 Figure 15. (a) Soil organic carbon content (% soil weight) within each sub-basin; (b) relation between the
 1157 parameter α in DOC equation (Equation 1) and the average soil organic carbon content of the drainage
 1158 area of each station; (c) relation between the parameter β in DOC equation (Equation 1) and the mean
 1159 annual discharge (Q) of each station; (d) relation between the parameter a in POC equation (Equation 2)
 1160 and Chl-a ($\mu g L^{-1}$; Le et al., 2017a); (e) relation between the parameter b in POC equation (Equation 2)
 1161 and the average soil organic carbon content of the drainage area of each station.

1162

1163



1164

1165 Figure 16. Comparison between observed and simulated discharge (top; mm.yr^{-1}) and
 1166 mg.L^{-1}). Coloured circles correspond to dates where DOC or POC data are available.

1167

1168

1169 Table 1. Values of the parameters α and β for dissolved organic carbon (DOC, Equation 1) and of the
 1170 parameters a, b, and %POC_{max} for particulate organic carbon (POC, Equation 2) at different stations, and
 1171 number (N) of sampling data (DOC and POC) used to calibrate the parameters.

Variables	Parameter	Yen Bai	Vu Quang	Hoa Binh	Son Tay
DOC	N (DOC)	94	94	96	73
	α (mg L ⁻¹)	4.5	5.0	5.5	5.0
	β (mm d ⁻¹)	0.7	0.8	1.7	2.5
	R ² (DOC concentrations)	0.04	0.00002	0.02	0.0001
POC	N (POC)	63	58	54	49
	a (mg L ⁻¹)	40.0	7.0	5.0	20.0
	b (%)	1.0	1.5	1.7	1.5
	%POC _{max}	10	15	40	15
	R ² (POC concentrations)	0.07	0.02	0.06	0.38

1172

1173 Table 2. Impacts of the new dams on the organic carbon dynamics (in kt.yr⁻¹) in the main tributaries of the
 1174 Red River. The values in parentheses represent the contribution of the three main tributaries.

Variables	Period	Yen Bai	Vu Quang	Hoa Binh	Son Tay
POC	2003-2007	490 ± 66 (69%)	132 ± 8 (19%)	87 ± 10 (12%)	662 ± 66
	2008-2013	175 ± 93 (71%)	43 ± 14 (18%)	28 ± 12 (11%)	193 ± 75
	Difference	-64 %	-67%	-68%	-71%
DOC	2003-2007	44 ± 7 (24%)	53 ± 3 (29%)	88 ± 12 (47%)	222 ± 18
	2008-2013	42 ± 20 (24%)	56 ± 16 (31%)	80 ± 34 (45%)	216 ± 79
	Difference	-5 %	+5%	-9%	-3%

1175

Table 3. Comparisons of organic carbon concentrations and fluxes between the present study and other studies in the Red River and in other rivers

River	Station	Drain Area (10 ³ km ²)	Period	DOC			POC			Reference
				Concentration (mg L ⁻¹)	Flux (kt yr ⁻¹)	Specific Yield (kg km ⁻² yr ⁻¹)	Concentration (mg L ⁻¹)	Flux (kt yr ⁻¹)	Specific Yield (kg km ⁻² yr ⁻¹)	
Red	Yen Bai	48.50	2008-2009	1.9	47	969	24.7	274	5649	Dang, 2006
				2.2	44	866	2.6	59	1258	Le et al., 2017a
				-	46	-	-	197	-	LOADEST (this study)
				1.51	59	1216	5.21	253	5216	This study
			2003-2013	1.39	44	907	8.35	318	6557	This study
	Vu Quang	30.37	2008-2009	2.4	78	2568	1.8	84	2766	Dang, 2006
				1.9	49	1613	0.8	47	1218	Le et al., 2017a
				-	59	-	-	50	-	LOADEST (this study)
				1.77	69	2272	1.33	55	1811	This study
			2003-2013	1.50	53	1745	2.30	83	2733	This study
	Hoa Binh	52.78	2008-2009	2.3	131	2482	1.3	55	1042	Dang, 2006
				1.7	82	1497	0.5	54	758	Le et al., 2017a
				-	98	-	-	58	-	LOADEST (this study)
				1.84	119	2255	0.62	40	758	This study
			2003-2013	1.60	88	1667	0.96	55	1042	This study
	Son Tay	137.23	2008-2009	2.5	263	1916	3.95	243	1771	Dang, 2006
-				286	-	-	259	-	LOADEST (this study)	
2.03				296	2157	1.66	255	1858	This study	
		2003-2013	1.81	222	1618	3.03	406	2959	This study	
Mekong	My Thuan (DOC) Phnom Penh (POC)	795	1972-1998 (DOC) 2006 (POC)	n.a.	2200	2767	2.01	1670	2100	Li et al., 2013 Ellis et al., 2012
Pearl	n.a.	452	2005-2006	1.7	380	840	1.5	540	1195	Ni et al., 2008
Yangtze	Datong	1830	2009	2.03	1580	863	n.a.	1520	831	Wang et al., 2012
Godavari	Rajahmundry	313	2003-2005	1.24	130	415	n.a.	756	2414	Balakrishna et al., 2006
Yellow	Lijin	752	2008-2012	3.3	60	80	1.39	410	545	Ran et al., 2013
Amazon	Obidos	6000	1994-2000	7.18	26900	4483	0.85	5800	967	Moreira-Turcq et al., 2003
Congo	Kinshasa-Brazzaville	3700	2009-2010	9.2	12480	3373	1.46	1960	530	Spencer et al., 2016

Table 4. The percentage of particulate organic carbon (POC) in total organic carbon (TOC) in two periods (before and after the new dam constructions) at each station

Variables	Period	Yen Bai	Vu Quang	Hoa Binh	Son Tay
POC/TOC	2003-2007	91%	72%	47%	74%
	2008-2013	81%	44%	26%	47%